The influence of modified gravitational theories on motions of Keplerian objects within the Solar System

Michael Sokaliwska

July 13, 2009

WIDMUNG

Contents

1 Introduction

There are a lot of mysteries in modern astrophysics that physicists were not able to solve up to now. One of these riddles is the so called Pioneer-Anomaly which seems to be an anomalous, mainly constant, acceleration of the two Pioneer space-crafts, directed to the Sun. This acceleration of the order of $10^{-10}\frac{m}{sec^2}$ has been observable over a distance between 20-70 AU, before the last signals have been received.
In order to find a solution to this problem, which turned out to be not explanable by error sources like technical errors, Solar wind influence or the gravitational influence due to the outer planets (Anderson et. al. [14]), the idea arrived that modifications of gravitation could solve this phenomenon.
Two of these modifications are the "Modified Newtonian Dynamics" (MOND) and the possibility of a suggestive Halo of Dark-Matter that is bound to the Solar-System. Both ideas turned out to be not sufficient in order to describe the deviations from expectations that have been observed, at least not at such distances where the Pioneer-Anomaly has been observed.

Not before heliocentric distances of the order of $10^4 - 10^5$ AU an observable influence can be expected. These are the distances where one suggests a reservoir of comets, the Oort Cloud.
This cloud or exactly the corresponding objects are the main subject of consideration in this thesis. Starting with the analysis of the influence of a special form of Vacuum-energy that has been derived by Fahr and Siewert, it will be investigated how the different modifications of gravity would influence the orbits of such objects under the assumption that they would move on circular orbits in the case of a pure Keplerian potential.

2 Perturbed space-time metrics: The influence of an alternative local spacetime-metric

2.1 Summary

In this chapter it will be investigated how a perturbed local spacetime metric could influence Keplerian Orbits. At first an equation will be derived and justified that describes the behaviour of an object in a locally contracting Robertson-Walker-like space-time metric used for our Solar System. For this local metric it turns out that metrical forces do not lead to measurable perturbations of Keplerian orbits.

2.2 Introduction

In modern cosmology the universe with its extension and masses is treated with the so called Robertson-Walker metric (RW-metric),

$$ds^2 = c^2dt^2 - a^2(t)(dr^2 + r^2(dr^2 + sin^2\theta d\phi^2)),$$

where a is the scale parameter of the universe, c the velocity of light, r the distance and dt an infinitisimal time-interval. θ and ϕ denote the polar and the azimute-angle. This metric leads to exact solutions for the Einstein Field equations and describes the homogeneously matter-filled and isotropically curved expansion or contraction of the universe.

For the metric of bound systems , e.g. like our Solar System, there is assumed to be some kind of static metric that does not participate in any kind of change of scale factor. This metric generally is taken to be the so called outer Schwarzschild metric. Obviously the local outer Schwarzschild metric must be somehow embedded into the global cosmic RW-metric and so defines a boundary layer between the static Schwarzschild-metric and the outer Robertson-Walker-metric. This region is called the Einstein-Straus vacuole (Einstein, Straus 1948).

However, this concept leads to fundamental problems. The main problem is the radius of such a vacuole. The vacuole for our Solar System would be of the order of about 120 pc. Within this radius there are a lot of other stars which also have an Einstein-Straus vacuole of this order of magnitude. So if this assumption is correct there should be very large regions in the universe with a non-defined metric due to the overlap of many ES-vacuoles, where also no cosmological redshift, one of the most used observational quantities in modern astronomy, can be expected. Thus one has to try another concept. This concept will be discussed in the following.

2.3 The concept of a local Robertson-Walker-metric

2.3.1 Mass growth within a bubble of local spacetime

As mentioned above the concept of the Einstein-Straus vacuole is not satisfactory. Since one considers scales of the order of our Solar System it seems convenient to take a closer look on the metrical dynamics and the growth of masses on scales where the local dynamics differs from global spacetime dynamics.

This was done by Fahr and Siewert (2007) [1] by allowing non-linear structure growth and justified the assumption of a different dynamical behaviour of a local scale compared with the global one.
So the local space time metric will "carve out" a vacuole-like region where the cosmic expansion does not take place; at least not as in the residual global universe.

2.3.2 Differential equation of motion on the local scale

Our Solar System is embedded in a global metric that is assumed to be a RW-metric and so should somehow be part of cosmic expansion.
There have been a lot of investigations how the global cosmic expansion could influence the dynamics within the Solar System [1],[3],[4]. To investigate this influence Cooperstock [3] derived an equation of motion for a particle in a gravitational force field which is also subjected to a global expansion of the surrounding universe. It is obvious that the expansion would lead to a repulsive force, if $\ddot{a}$ is positive, seen from the centre of the gravitational field. This equation is given by

$$\frac{d^2x}{dt^2} = -\frac{GM}{x^2} + \frac{\ddot{a(t)}}{a(t)}x, \tag{1}$$

where x describes the distance from the centre, G is Newtons gravitational constant and M the central gravitating mass. The first term on the RHS results from the attractive gravitational field whereas the second term corresponds to a repulsive force connected with the global expansion.
It is justified to suppose that the global expansion will not lead to a measurable effect at small distances (See Fahr and Siewert, 2007a,b). But at the border of the region of the local metric, the influence may not be negligible. To see how a local scale parameter could behave in such a field, Fahr and Siewert chose a distance that correpsonds to the local scale length l. The region within radius can be described by a different metrical behaviour. What they got, was an equation of motion for the local scale parameter l

$$\ddot{l}(t) = -\frac{GM}{l^2(t)} + l(t)\frac{\ddot{a}(t)}{a(t)}. \tag{2}$$

This second order differential equation can be transformed into a first-order one by multiplying with $2\dot{l}$ which leads to

$$\tfrac{d}{dt}\dot{l}^2(t) = 2\tfrac{d}{dt}\tfrac{GM}{l} + \tfrac{\ddot{a}}{a}\tfrac{d}{dt}l^2.$$

It can formally be integrated using a relation also derived by Fahr and Siewert [2],[1] (see Appendix in [1]) and leads to

$$\dot{l}^2 = 2GM\left(l^{-1} - l_{rec}^{-1}\right) + \frac{1}{2}\left(\frac{\ddot{a}}{a} + \frac{\ddot{a}_{rec}}{a_{rec}}\right)\left(l^2 - l_{rec}^2\right) + \dot{l}_{rec}^2. \tag{3}$$

Solving this equation in its general form needs numerical methods and is not trivial. So it is convenient to analyze the asymptotic behaviour of this equation. At first they considered the case that the scale factor l at time t is much larger than the associated scale factor at recombination time, $l(t) \gg l_{rec}$. Then the above equation reduces to

$$\dot{l}^2 = -\frac{2GM}{l_{rec}} + \frac{1}{2}\left(\frac{\ddot{a}}{a} + \frac{\ddot{a}_{rec}}{a_{rec}}\right)l^2 + \dot{l}_{rec}^2. \tag{4}$$

The RHS of this equation must always be positive and leads to the condition

$$\frac{2GM}{l_{rec}} < \frac{1}{2}\left(\frac{\ddot{a}}{a} + \frac{\ddot{a}_{rec}}{a_{rec}}\right) l^2 + \dot{l}_{rec}^2.$$

This condition suggests that, if it is fullfilled, a region of gravitationally bound spacetime may only grow large if the central mass is sufficiently small. Another interpretation is that in conflict with the radius of an Einstein-Straus vacuole the region where the dynamical influence of the attractive force exceeds the cosmological force is not as large as expected from the Einstein-Straus vacuole.

In the opposite case, $l(t) \ll l_{rec}$, the equation of motion of the local scale factor yields

$$\dot{l}^2 = -\frac{2GM}{l} - \frac{1}{2}\left(\frac{\ddot{a}}{a} + \frac{\ddot{a}_{rec}}{a_{rec}}\right) l_{rec}^2 - \dot{l}_{rec}^2, \tag{5}$$

which leads to the condition

$$\frac{2GM}{l} + \dot{l}_{rec}^2 > \frac{1}{2}\left(\frac{\ddot{a}}{a} + \frac{\ddot{a}_{rec}}{a_{rec}}\right) l^2,$$

and can be interpreted in that way that a sufficiently large central mass causes an asymptotically small vacuole.

2.3.3 Mathematical structure

To investigate the mathematical structure of the above derived equation of motion one can make use of the well-known relations which follow from the conventional Friedmann equations in a matter-dominated, pressure-less universe

$$\begin{aligned} a(t) &= a_{rec}\left(\frac{t}{t_{rec}}\right)^{2/3}, \\ \dot{a}(t) &= \frac{2}{3}\left(\frac{a(t)}{t_{rec}}\right)\left(\frac{t}{t_{rec}}\right)^{-1} = \frac{2}{3}\frac{a(t)}{t}, \\ \ddot{a}(t) &= -\frac{2}{9}\left(\frac{a(t)}{t_{rec}^2}\right)\left(\frac{t}{t_{rec}}\right)^{-2} = \frac{2}{9}\frac{a(t)}{t^2}, \end{aligned} \tag{6}$$

and (3) then becomes

$$\dot{l}^2 = 2GM\left(l^{-1}(t) - l_{rec}^{-1}\right) - \left(l^2(t) - l_{rec}^2\right)\left(\frac{1}{9t_{rec}^2} + \frac{1}{9t^2}\right) + \dot{l}_{rec}^2.$$

By approximating $\dot{l}_{rec}$ by $\frac{\dot{a}_{rec}}{a_{rec}} = \frac{\dot{l}_{rec}}{l_{rec}}$ and replacing $\dot{a}_{rec}$ by $\dot{l}_{rec}$ one gets

$$\dot{l}^2 = 2GM\left(l^{-1} - l_{rec}^{-1}\right) - \frac{l^2(t) - l_{rec}^2}{9t_{rec}^2}\left(1 + \frac{t_{rec}^2}{t^2}\right) + l_{rec}^2\left(\frac{2}{3t_{rec}}\right)^2.$$

Dividing this expression by $l^2(t)$ delivers an equation which looks quite similar to the Friedmann-Lemáitre equation,

$$\left(\frac{\dot{l}}{l}\right)^2 = \frac{\alpha}{l^3(t)} + \frac{\beta(t)}{l^2(t)} + \gamma(t), \tag{7}$$

with the parameter functions

$$\begin{aligned} \alpha &= 2GM, \\ \beta(t) &= \left(\frac{2l_{rec}}{3t_{rec}}\right)^2 - \frac{2GM}{l_{rec}} + \frac{l_{rec}^2}{9t_{rec}^2}\left(1 + \frac{t_{rec}^2}{t^2}\right), \\ \gamma(t) &= -\frac{1}{9t_{rec}^2}\left(1 + \frac{t_{rec}^2}{t^2}\right). \end{aligned} \tag{8}$$

Although the above equation bears a strong reminescence to the Friedmann-Lemáitre equation, there are some important differences:
The first term on the RHS corresponds to the cosmological mass density term; the second term with $\beta(t)$ seems to correspond to the curvature term with the difference that this curvature is time-dependent here. The last term corresponds to a vacuum energy term, but seems to be negative and time-dependent. In a further chapter this special result will be investigated, with respect to whether or not this term is sufficient to cause deviations of Keplerian orbits from expectations.

2.3.4 A special solution

The question now is: How does the local scale factor behave with time? To investigate this interesting point Fahr and Siewert derived specific solutions for $l(t)$. In order to do this, they considered the case where $l \gg l_{rec}$ under the initial condition that at the recombination phase, the following boundary condition is valid

$$\dot{l}_{rec}^2 - \frac{2GM}{l_{rec}} = 0, \tag{9}$$

which means that at the so defined boundary layer, at recombination-time t_{rec}, the gravitational binding energy of the mass inside the local bubble is equivalent to the kinetic energy of expansion, and thus leads to

$$\frac{\dot{l}}{l} = \pm\sqrt{\frac{1}{2}\left(\frac{\ddot{a}}{a} + \frac{\ddot{a}_{rec}}{a_{rec}}\right)}, \tag{10}$$

where the plus-sign is used for times $t \leq t_0$ and the minus-sign for times $t \geq t_0$. t_0 denots the time when the expansion of the local-spacetime stops. This differential euqation has the following solution, with $\dot{l}(t_0) = 0$

$$l(t) = l_0 exp\left[-\int_{t_0}^{t}\sqrt{\frac{1}{2}\left(\frac{\ddot{a}}{a} + \frac{\ddot{a}_{rec}}{a_{rec}}\right)}dt\right]. \tag{11}$$

For a universe with dominant and constant vacuum energy density $\rho_\Lambda c^2$ the following solution for the cosmic scale parameter is obtained (Harrison 1988) [5]:

$a = a_0 exp[H_\Lambda(t - t_0)]$,

with $H_\Lambda = \sqrt{8\pi G\rho_\Lambda/3}$.

Using this relation leads to

$$l = l_0 exp[-H_\Lambda (t - t_0)]. \tag{12}$$

This indicates a local spacetime contraction with time rather than an expansion.

The above solution seems to be in conflict with the assumption of $l \gg l_{rec}$. But at the beginning of structure formation the local scale first continues to grow like a up to a limit of $\dot{l} \leq 0$. Up to this point l may have grown up to $l \gg l_{rec}$ and than turns over to contraction.

2.3.5 The meaning of a contracting local scale parameter l

The consideration of the behaviour of a local scale factor for our Solar System leads to a $l(t)$ which decreases with time. It should be noted here that l describes in the end the shrinking of the radius of the local spacetime area with a different metric than the cosmic one. A full description of a contracting spacetime within gravitationally bound systems may lead to a distance-dependent scale parameter $l(t)$ and a very difficult to obtain quantity.
The idea of this concept is basically to describe a local Roberston-Walker-like metric with a local scale parameter. The problem with such a metric is that a RW-metric needs an isotropic and homogeneous mass-density-distribution, which is obviously not the case within the Solar-System. So redistributing the central mass into a homogeneous density-distribution is required.

2.3.6 Metrical attractive forces due to a contracting local scale

In the framework of the foregoing section, a local RW-like metric behaves as a contracting metric with a scale factor $l(t)$ which has the form

$$l = l_0 exp[-H_\Lambda (t - t_0)].$$

From this it is trivial to get the quotient

$$\frac{\ddot{l}}{l} = H_\Lambda^2.$$

At the very beginning of this part of the chapter equation (1) derived by Cooperstock (1998) was presented,

$$\frac{d^2 r}{dt^2} = -\frac{GM}{r^2} + r\frac{\ddot{a}(t)}{a(t)},$$

which describes how the cosmic expansion is acting on a particle in a gravitational force field. But how does the local contraction influence the motion of this particle?
If one treats now the local scale factor l, with its contraction corresponding to the expanding global scale factor a, the above equation becomes

$$\frac{d^2 r}{dt^2} = -\frac{GM}{r^2} - r\frac{\ddot{l}(t)}{l(t)}. \tag{13}$$

Where the minus sign results from , the vector-orientation of $\ddot{l}$ which correspond to an attractive behaviour of the metrical term $\frac{\ddot{l(t)}}{l(t)} r$.

Obviously the gravitational potential may be somehow modified due to a contribution of the local contraction. To deduce whether or not there can be any measurable contribution to the effective force field, the radius up to which the metrical force $-{H_\Lambda}^2 r$ can be neglected was calculated. For this it is neccesary to investigate where the two different forces become of the same order of magnitude, i.e.

$$\frac{GM}{r^2} = r\frac{\ddot{l}(t)}{l(t)}.$$

This leads to the following expression for the critical radius,

$$r_{crit} = \left(\frac{GM}{\ddot{l}(t)/l(t)}\right)^{\frac{1}{3}} = \left(\frac{GM}{H_\Lambda^2}\right)^{\frac{1}{3}}. \tag{14}$$

After plugging numbers (i.e. $H_\Lambda = 73 km/s/Mpc$) the critical radius turns out to be of the order of $r_{crit} \approx 10^2 pc$ or $r_{crit} \approx 300 ly$. The Oort cloud, that is assumed to define the last 'material' border of our Solar System, in fact lies in a distance of about 1 light year. At such distances the contribution of metrical forces, relative to the Keplerian force, is about 0.0000033 percent.
On the basis of present-day believed values of cosmic vacuum energy density this excludes any recognition of a metrical effect on Solar System bodies.

2.4 Conclusions

In this chapter the possible influence of a locally contracting spacetime scale l, in analogy to an expanding global Robertson-Walker metric, has investigated. Starting from a non-linear density growth it turned out that the Solar System can be treated with a local RW-metric (redistributing the central mass) in contrast to the Einstein-Straus-vacuole concept. The behaviour of the local scale factor of this bubble with time leads to a contracting local metric which should contribute an additional attractive term in the equation of motion (Cooperstock, 1998). It turned out that the critical radius at which the contributions of the gravitational field and the metrical force from contraction are essentially equal, is many orders of magnitude too large to induce any influence from local scale contraction on Keplerian objects within our Solar System. Even Oort cloud objects would not feel any influence from this contribution.

2.5 Further investigations

Although the last investigation showed that metrical forces are not sufficient to cause any measurable effect on motions within the Solar System it should be mentioned that this only applies to the assumed present day value for the Hubble-constant, H_Λ. If we take some other ideas into account, e.g. that the vacuum-energy density is NOT a constant the above consideration has to be repeated. In [7] and [8] the possibility of a vacuum-energy density which decreases with increasing cosmic scale, was discussed. Assuming this is true the question remains how the vacuum-density behaves on local, contracting, scales, that decoupled from cosmic expansion.

When the local scale turns over from expansion to contraction and so decouples from the cosmic expansion, the vacuum-energy density may also decouple

and not decrease further. It may stay constant or even increase again, as required for an economic universe (see Fahr and Heyl, 2007). The so developed value for the 'local Hubble-constant' may be completely different from the one assumed above and so may lead to an influence on motions within the Solar System. However, to take this into account it will be necessary to analyze the time evolution of the vacuum-energy on cosmic and local scales.

Furthermore the assumption of a contracting scale factor that contracts equally at every distance is just an idealized model. At the border of the sphere, limiting the local contracting metric, the rate of contraction should behave very different than at smaller distances, because of the contribution of cosmic expansion. Taking this into account could also lead to different results.

3 The possible influence of a negative time-dependent Cosmological Constant within the Solar System

3.1 Summary

In the foregoing chapter the influence of a contracting local Robertson-Walker like metric on Keplerian objects within the Solar System has been investigated. It could be excluded that such a local contraction would have any measurable influence on the pathways of objects within the Solar System, even if we take the Oort cloud with a distance of about 1 lightyear into account. In the framework of this investigation an equation was derived that looks similar to the well known Friedmann-equation. In this equation a term appeared which corresponds to the cosmological constant Λ, but is dependent on time and is negative.
The following section will investigate, under what conditions such a negative time-dependent cosmological term cannot be neglected anymore and how it would contribute to motions of Keplerian objects within the Solar System.

3.2 A locally-valid cosmological constant Λ_-

In the foregoing chapter the equation (1) derived by Cooperstock [2] was used, describing the impact of expansion of the universe on the dynamics within the Solar System,

$$\frac{d^2r}{dt^2} = -\frac{GM}{r^2} + r\frac{\ddot{a}}{a}.$$

If one uses this equation as the equation of motion of an object at a central distance l one obtains (Fahr, Siewert 2008)

$$\frac{d^2l}{dt^2} = -\frac{GM}{l^2} + l\frac{\ddot{a}}{a}.$$

From this Fahr and Siewert [1] derived an equation for the special case of $l \gg l_{rec}$ which has the mathematical form of the Friedmann-equation,

$$\left(\frac{\dot{l}}{l}\right)^2 = \frac{\alpha}{l^3(t)} + \frac{\beta(t)}{l^2(t)} + \gamma(t),$$

with the parameter functions

$$\begin{aligned} \alpha &= 2GM, \\ \beta(t) &= \left(\frac{2l_{rec}}{3t_{rec}}\right)^2 - \frac{2GM}{l_{rec}} + \frac{l_{rec}^2}{9t_{rec}^2}\left(1 + \frac{t_{rec}^2}{t^2}\right), \\ \gamma(t) &= -\frac{1}{9t_{rec}^2}\left(1 + \frac{t_{rec}^2}{t^2}\right). \end{aligned} \tag{15}$$

As one can see, the last term $\gamma(t)$ corresponds mathematically to the cosmological constant in the Friedmann-equation, and has the dimension of $\frac{1}{s^2}$. If one devides it by the square of velocity of light it yields

$$\Lambda_- = \frac{\gamma(t)}{c^2}$$

The equivalent of the "cosmological constant" seems to be today ($t = 13,7 \times 10^9 yrs$ and $t_{rec} = 3 \times 10^5 yrs$)

$$\Lambda_- = -1.38 \times 10^{-44} \frac{1}{m^2},$$

which is three orders of magnitude larger than the upper limit for the present-day usual cosmological constant Λ.
Such a cosmological constant is very suggestive. It would lead to an additional attractive term in the potential and furthermore correspond to a negative, local vacuum energy density $\rho_{vac}^- = -\frac{\Lambda_- c^2}{8\pi G}$.

3.3 The vacuum-modified potential

Although the value for the negative cosmological constant[1] is small, it nevertheless may have an influence like an attractive force on the motion of bodies within the Solar System. As derived in [6] the force that is acting on a particle, taking the influence of the vacuum into account, is given by

$$\ddot{r} = -\frac{GM}{r^2} + \frac{c^2 \Lambda}{3} r, \tag{16}$$

or rather in the case here,

$$\ddot{r} = -\frac{GM}{r^2} + \frac{c^2 \Lambda_-}{3} r, \tag{17}$$

where Λ_- is the above negative constant which leads to an additional attractive force towards the centre. From this one can derive the corresponding potential via $-\frac{\partial \Phi(r)}{\partial r} = F(r)$,

$$\Phi(r) = -\frac{GM}{r} - \frac{c^2 \Lambda_-}{6} r^2 + const. \tag{18}$$

The attraction of this potential increases with increasing distance $\propto r^2$. How this potential looks like is shown in Figure 1 where also the normal gravitational potential is plotted.

A comparsion of the two contributions, the gravity force and the (negative) vacuum force is shown in Figure 2.

3.4 The critical radius

To have an idea of the power and range of the impact of the negative vacuum energy it is necessary to calculate the radius at which both forces, the gravitational force and the force due to Λ_- are equivalent and so have the same order of magnitude.

The force due to the negative vacuum energy density is $\frac{c^2 \Lambda_-}{3} r$. Since Λ_- is negative the induced force is directed towards the centre, just as the gravitational force.
The above expression leads to the condition for the critical radius,

$$r_{crit} = \left(\frac{3GM}{c^2 \Lambda_-} \right)^{\frac{1}{3}}. \tag{19}$$

[1] $\gamma(t)$ stays mainly constant today

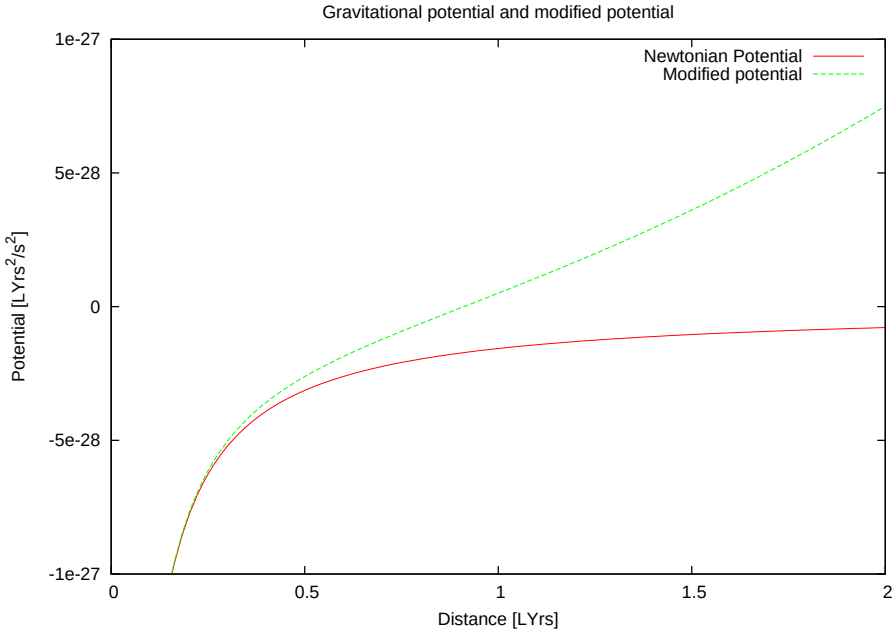

Figure 1: Gravitational potential and vacuum modified potential

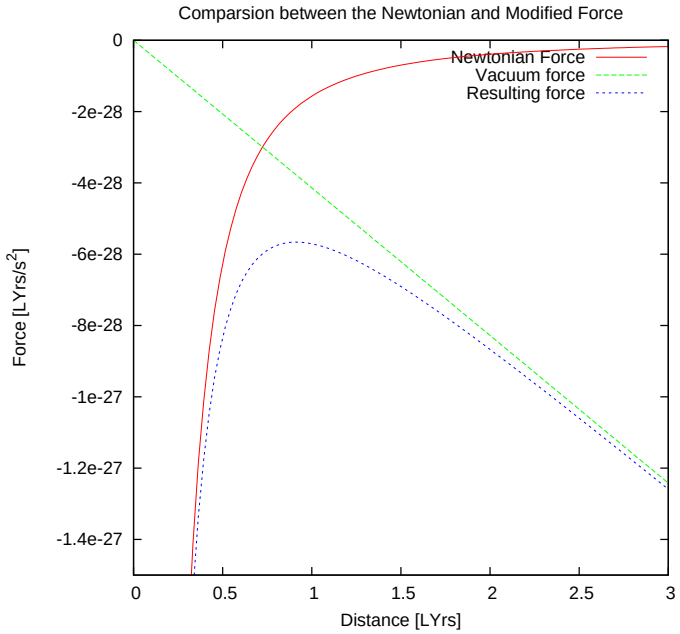

Figure 2: Comparsion between the Gravitational force and the vacuum induced force

It turns out that this radius is about $r_{crit} \approx 7 \times 10^{15} m \approx 7 \times 10^{-1} Lyr = 4,6 \times 10^4 AU$. At this distance the influence of the vacuum can not be neglected

anymore, or, in other words, it is not possible to use perturbation theory because the "perturbation" is neither small nor time limited on a small interval. By comparsion, the general cosmological constant with an upper limit of $10^{-47}\frac{1}{m^2}$ would lead to a critical radius of about 8 Lys.

Obviously a distance of 0.7 Lys is too large to expect a direct influence on the pathways of planets within the inner Solar System. But if one takes the Oort cloud into account which is about 1 Ly away it should be possible to see some deviations from pure Keplerian expectations.

3.5 Mathematical consideration: Celestial mechanics

In the foregoing section the radius has been derived, where the influence of the gravitational force due to the central mass and the force due to negative vacuum energy-density become of the same order of magnitude. It turned out that this radius is smaller than 1 Lyr, thus it is worthwhile to take a closer look on the possible influence. Differently from the "normal" positive cosmological constant the negative one acts as an additional, attractive force and so has to be taken into account in the derivation of the equation of motion for an object in this modified potential.

In celestial mechanics the possible orbits within a central potential can be derived by using the Lagrangean in polar coordinates,

$$L = \frac{m}{2}\left(\dot{r}^2 + r^2\dot{\phi}^2\right) - V(r),$$

where $V(r)$ denotes the potential energy of the particle. This leads to an equation for the angle ϕ as a function of distance r,

$$\phi(r) = \pm\frac{p_\phi}{m}\int \frac{dr'}{r'^2\sqrt{\frac{2}{m}\left[E - V(r) - \frac{p_\phi^2}{2mr'^2}\right]}} + \phi_0,$$

with the constant angular momentum $p_\phi = mr^2\dot{\phi}$. Usually one can integrate analytically this equation if the potential has the form $V(r) = -\frac{\alpha}{r}$. But this is obviously not the case here. For distances where the negative vacuum density is no longer negligible the additional term $-\frac{c^2\Lambda_-}{6}r^2$ has to be inserted into the above equation. Doing this leads to

$$\phi(r) = \pm\int \frac{dr'}{\sqrt{\frac{2mc^2\Lambda_-}{p_\phi^2}r'^6 + \frac{2mE}{p_\phi^2}r'^4 + \frac{2m\alpha}{p_\phi^2}r'^3 - r'^2}}. \tag{20}$$

This equation has the form

$$I(x) = \int \frac{dx}{\sqrt{ax^6+bx^5+cx^4+dx^3+ex^2}},$$

and has to be integrated numerically. The question is: Does this solution lead to Keplerian orbits?

Another possibility to consider the direct impact of Λ_- is to include it into numerical simulations. Using such a simulation should lead to the same qualitative results for the pathways, as the numerical integration of equation (20)

does. With this goal an orbit-integrating program designed by Michael Marks and Jan Pflamm-Altenburg was used. The results will be presented in the following.

3.6 The program

The critical radius where the gravitational force and the force due to the negative cosmological constant, Λ_-, become equivalent lies in a distance of about 0.7 Lys. To estimate the influence the additional force would have at such a distance, an orbit integrating programme[2], designed by Michael Marks and Jan Pflamm-Altenburg, was used. This program computes the mutual forces of bodies within a Keplerian potential.

The program was designed to investigate the possible influence of a suggestive Dark Mater halo within our Solar System (see Section 5). The goal of this program is to compute the forces and accelerations that act on the bodies.
Starting from an input file which contains the position- and velocity-components (x,y,z) of the planets and the Sun at a chosen time, the program is able to calculate, via the 'Runge-Kutta-method', the time evolution of the Solar System bodies. As one can see from the critical radius derived above there is no influence expected from Λ_- on the motion of the planets. Only at distances of the order of 40.000 AU a direct observable deviation from Keplerian orbits can be expected.

It is obvious that a bound object at such a large distance from the centre (the Sun) has a very long period. So it was necessary to choose appropriate time steps ($dt = 100 days$) in contrast to the smaller ones for planetary motions

After changing the time steps and the integration time, different initial conditions were chosen. Angular momentum conservation allows to perform the orbit integration in one plane, the x-y-plane[3]. Ten cases at different distances have been considered (see Table 1). For these, the initial conditions were chosen to deliver circular orbits in the pure Keplerian case. Two examples are ellipses.

The investigation was started with the case of a circular orbit within the unperturbed Keplerian potential. It should be mentioned here that the possible influence of a galactic tidal field or other external field sources were not taken into account in these calculations. The whole calculations (also for the two other cases considered in this thesis) just involve the isolated two-body-problem.
From celestial mechanics we know that for a circular orbit the condition,

$$E_{circle} = -\frac{\alpha}{2R},$$

has to be fullfilled. Where $\alpha = GmM$ is the gravitational constant times the masses of the two interacting objects and R is the radius of the circular orbit. From this the velocity-component follows,

$$-\frac{\alpha}{2R} = \frac{1}{2}mv^2 - \frac{\alpha}{R} \Rightarrow v = \sqrt{\frac{GM}{R}},$$

[2] A extraction from the source code is shown in the Appendix
[3] As mentioned in the following section, there is no change or dependence on inclination.

$GM[\frac{AU^3}{Day^2}]$	$x[AU]$	$y[AU]$	$z[AU]$	$v_x[\frac{AU}{Day}]$	$v_y[\frac{AU}{Day}]$	$v_z[\frac{AU}{Day}]$
0.22e-15	50000	0	0	0	0.000077	0
0.22e-15	48000	0	0	0	0.000079	0
0.22e-15	45000	0	0	0	0.000081	0
0.22e-15	40000	0	0	0	0.000086	0
0.22e-15	35000	0	0	0	0.000092	0
0.22e-15	30000	0	0	0	0.000099	0
0.22e-15	28000	0	0	0	0.000103	0
0.22e-15	25000	0	0	0	0.000109	0
0.22e-15	10000	0	0	0	0.000172	0
0.22e-15	5000	0	0	0	0.000243	0
0.22e-15	48000	0	0	-0.00004	0.000039	0
0.22e-15	20000	0	0	0	0.00001	0

Table 1: Initial conditions for the orbit integration: G is normalized to Solar masses

for different initial distances R.

At large distances the interaction of the planets can be neglected and the problem reduces to a two-body-problem, the central mass and the model object with the spatial coordinates $(X; 0; 0)$ with $(X = 50.000; 48.000; ...)$ and the velocity $\overrightarrow{v} = (0; v; 0)$.

3.7 Resulting orbits of objects within the Λ_--modified potential

To see how the negative cosmological constant Λ_- influences the motion of bodies within the Solar System at large distances the vacuum-induced force $\frac{c^2\Lambda_-}{3}r$ has been added into the calculation of the acceleration within the program. This force acts as an additonal attractive force and enhances the attraction of the central mass. So one would expect that objects that would follow a circular Keplerian orbit will deviate strongly from this path.

Indeed this is exactly what happens with the bodies at such distances. The orbit integration shows clearly how the force due to Λ_- acts. The following figures show the behaviour of objects that move in the modified potential. The solid line represents the expected orbit within an unperturbed Keplerian potential. The integration-time was chosen differently because for smaller distances the influence of Λ_- disappeared rapidly.

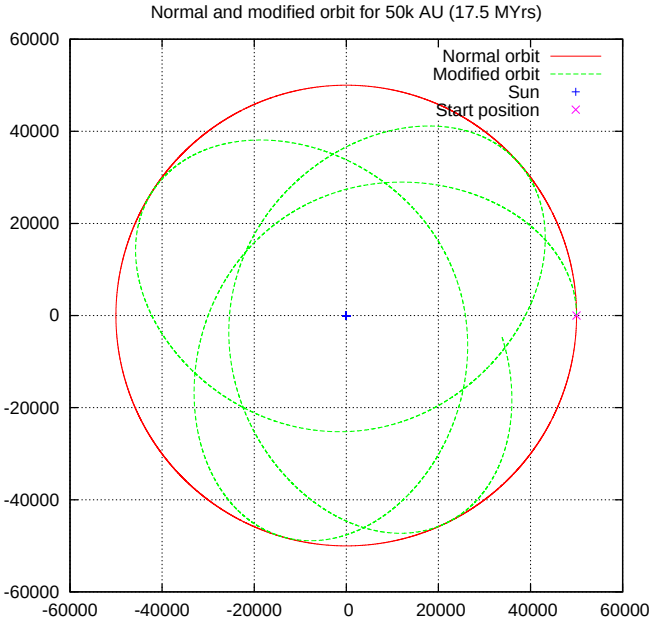

Figure 3: Resulting orbits for a distance of 50.000 AU

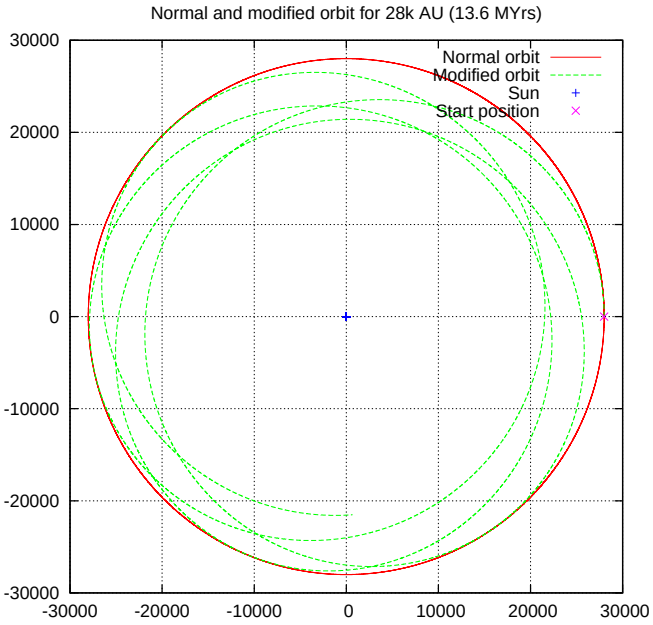

Figure 4: Resulting orbits for a distance of 28.000 AU

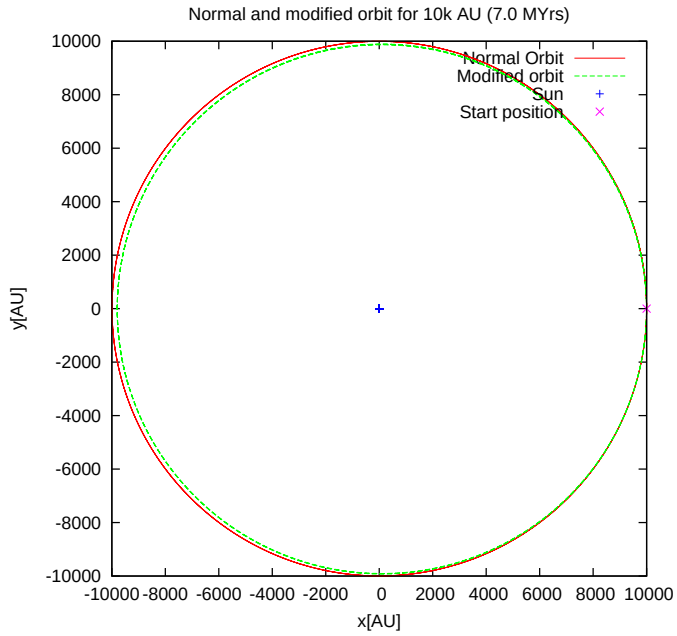

Figure 5: Resulting orbits for a distance of 10.000 AU

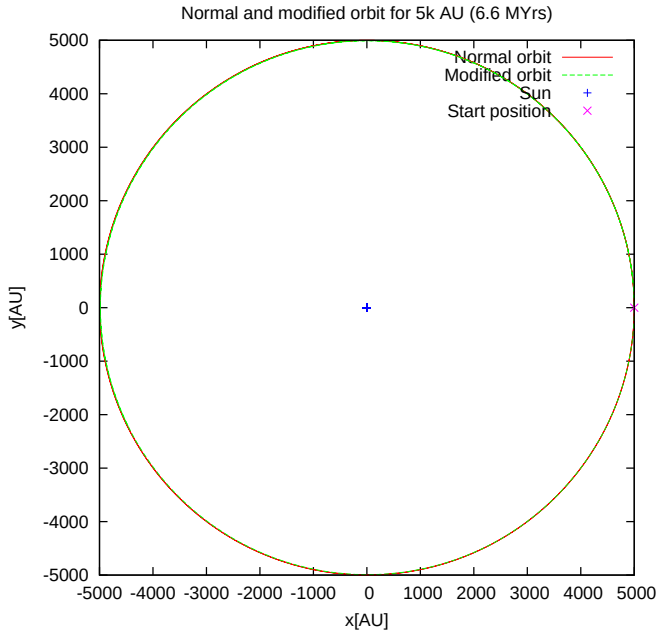

Figure 6: Resulting orbits for a distance of 5.000 AU

From these results one can see that objects that would follow a circular orbit are forced to move on an elliptical orbit due to the vacuum-force. The resultant ellipses additionally affect a turn of their perihelion. Furthermore it is obvious how the influence of Λ_- vanishes with decreasing distance.

Additionally there seems to be a lower limit for the minimum distance to the Sun. In the case of the orbit for 50.000 AU the perihelion lies at approximately 20.000 AU.

Some more illustrative expamples are given in the following. For these orbits different initial velocity components have been used in order to start from an elliptical Keplerian orbit. These orbits are also forced to change their orbital parameters. One can see the turn of the periphelion just as in the foregoing examples. And, additionally, a change in eccentricity is obvious.

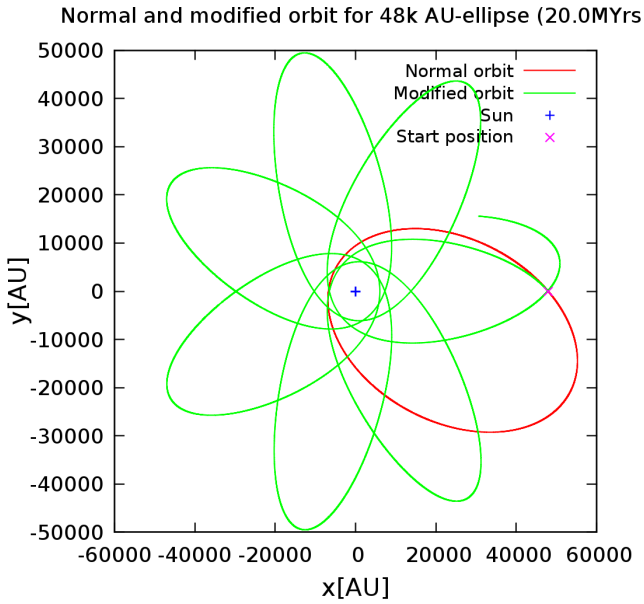

Figure 7: Resulting orbit for an elliptical orbit starting from 48k AU

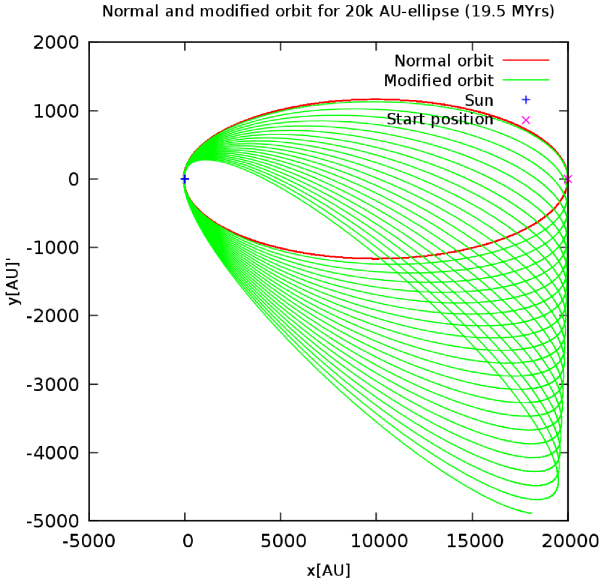

Figure 8: Resulting orbit for an elliptical orbit starting from 20k AU

The last orbit is the result of the initial conditions for a very high eccentricity ellipse. It seems that the eccentricity increases with every turn and no aphelion-turn is obvious. Foremost for longer integration time the turn of aphe-

lion is visible.

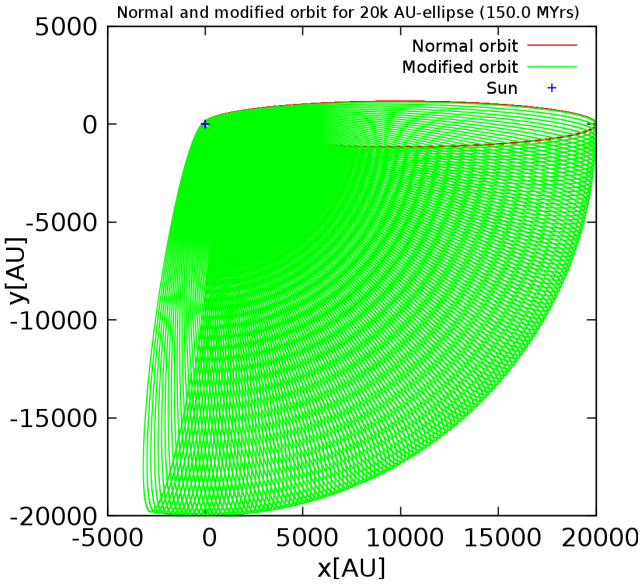

Figure 9: Resulting orbit for a high eccentricity ellipse at 20.000 AU (Integration-time 150 million years)

To learn more about the change of the orbital parameters it has been investigated, in the following section, how the semi-major axis and the eccentricity would behave, if the object, with the actual spatial and velocity components, would move within a Keplerian potential which one would assume if it would be possible to observe very long periodic Oort objects[4].

[4]Very long periodic means objects with an aphelion-distance of the order of 10^4 AU.

3.8 Change of orbital parameters

To get a more transparent view of what happens with objects within the Λ_--modified potential the orbital parameters for the resulting orbits have been considered.

For this, two kinds of parameters were introduced, the 'active orbital parameters' that describe the actual pathway of the test object within the modified potential, and the 'passive orbital parameters' that contain information about the resulting orbit of each point the particle runs through, under the assumption of an usual Keplerian potential. In other words these would be the orbital parameters one would expect to see for an observed Oort object.

3.8.1 Passive orbital parameters

For the analysis of the passive orbital parameters the case of an object at an initial distance of 50000 AU has been considered.

Semi-major-axis and aphelion-distance

To analyse how the semi-major axis a changes within the Λ_--modified potential the value of a for every point of the orbit has been calculated via

$$a = \frac{r}{2 - rv^2/\mu}, \tag{21}$$

- where r is the distance that changes with time, v the velocity and $\mu = GM$, with the actual $x-$ and $y-$components in space and velocity there, under the assumption of a motion within a normal Keplerian potential. So the following results correspond to 'best-fitting-orbits' for every point.

For an object within a Keplerian potential Figure 10 would show a straight line at the values of the corresponding semi-major axis and aphelion, whereas the object within the modified potential would move to very high distances in case of an idealized Keplerian orbit. The reason why such large values are not actually reached[5] is the additional attractive force due to Λ_-. Conspicuous are the oscillations, that develop in this case.
Comparsion with the velocity components shows (Figure 11) that the maximum value for a corresponds to the transit through the periphelion and the minimum to the transit through the aphelion. This results from the accelerations the body undergoes. Near the Sun the body already has a high velocity due to the attraction of the Λ_--force. Ignoring now the modification of the potential the body would fly to very large distances. When the acceleration towards the centre becomes too large the velocitiy decreases and the body turns its direction of motion. At this point the velocities are small and so would lead to a small semi-major axis.

Eccentricity

From the behaviour of the semi-major-axis it is obvious that one could expect

[5] As one can see in Figure 3

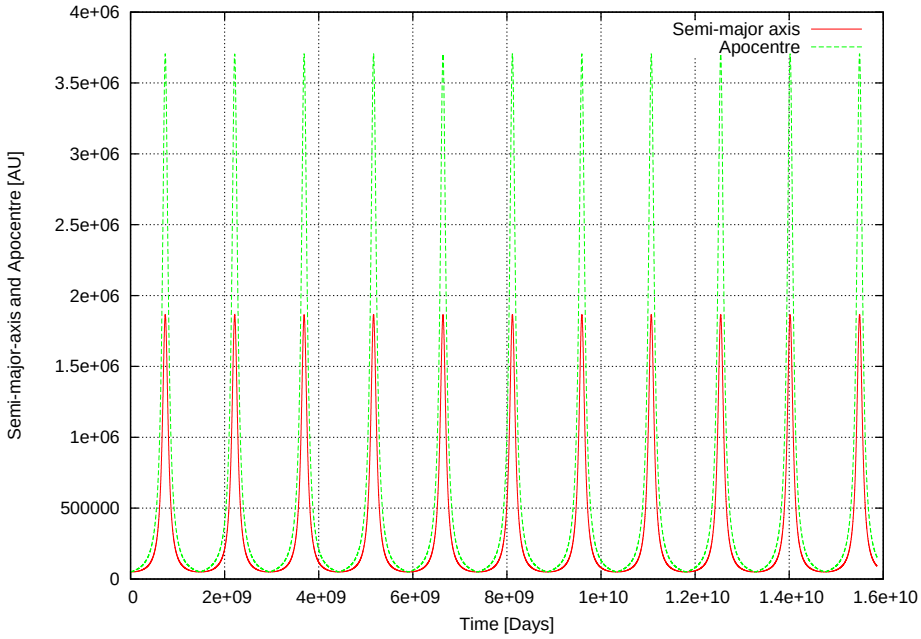

Figure 10: The behaviour of the instantaneous best-fitting semi-major-axis and the aphelion-distance with time

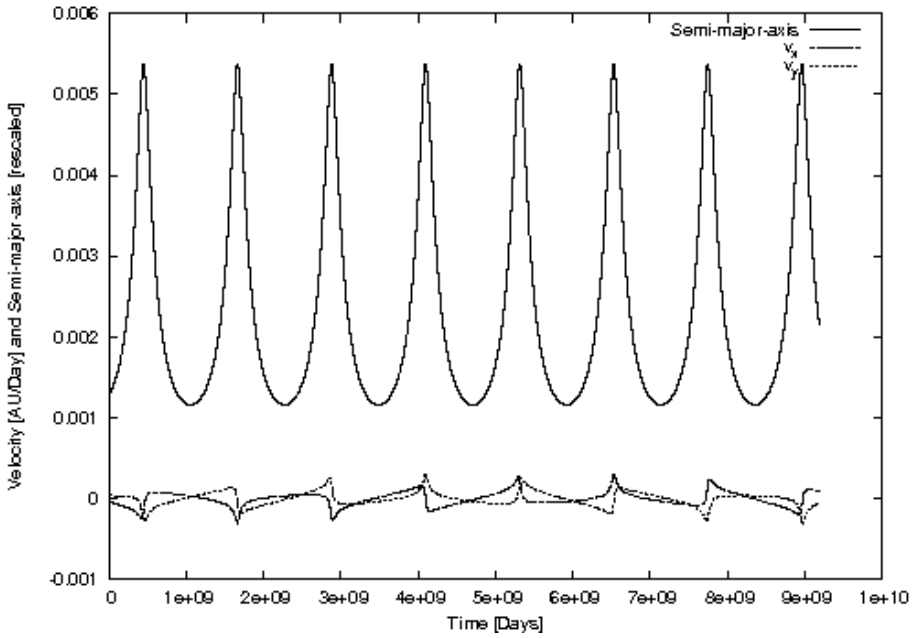

Figure 11: Time comparsion of semi-major-axis a and the velocity components.

very high eccentric but closed orbits with the used spatial and velocity components. This expectation is supported by the consideration of the eccentricity that the resulting orbits would have.
As for the calculation of the semi-major-axis for the best fitting orbit the eccentricity was calculated for each point. For this the following equation was used:

$$\epsilon = \sqrt{1 - \frac{p_\phi^2}{a\mu}}, \tag{22}$$

where p_ϕ is the conserved angular-momentum, a the semi-major-axis, calculated in the foregoing step and $\mu = G_N M_\odot$ the gravitational constant times the solar mass.
Figure 12 shows the resulting eccentricities. It is obvious that orbits with the whole spectrum of eccentricity can occur. Also pure circular orbits and very elliptic orbits[6].

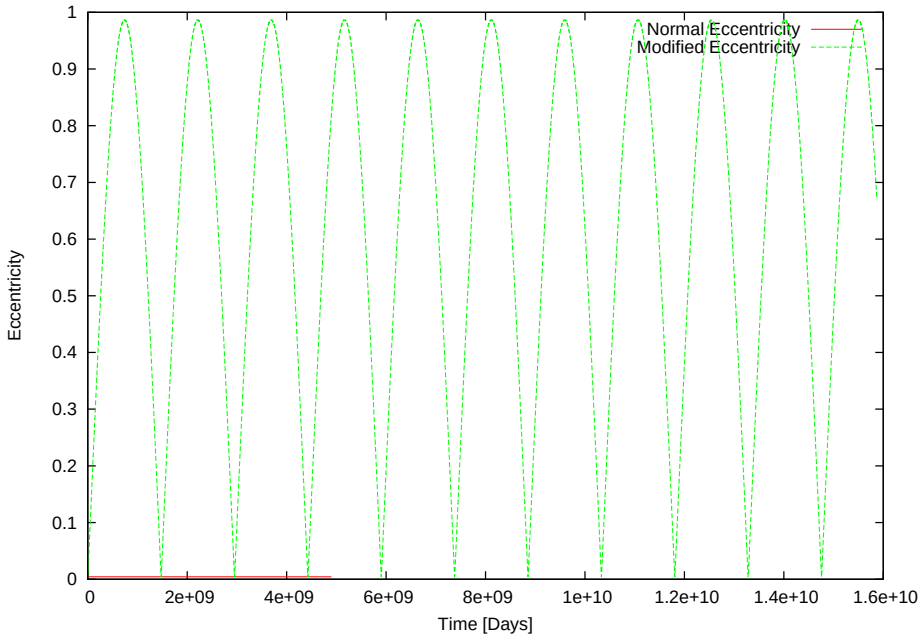

Figure 12: Change of eccentricity

The calculation of the passive orbital parameters delivers the parameters one would observe for objects originating from the Oort cloud and under the assumption of a classical Keplerian potential. If one could observe an object and compares the accordingly path-parameters for several points of time it should be possible to confirm or disprove the influence of a suggestive negative cosmological constant Λ_-. In order to do this, objects with very long period orbits

[6]The initial condition were chosen such that they would cause a circular orbit with eccentricity zero. The calculation of the eccentricities showed that this is not fully true. The initial orbit has a very low eccentricity of 0.004368. This is caused by uncertainties in constants, e.g. the gravitational constant or the Solar mass and maybe small numerical errors.

or, in other words at large distances from the Sun would be necessary.

3.8.2 Active orbital parameters

To give a full description of the influence of Λ_- also the actual behaviour of objects and their orbits within the modified potential has been investigated. For this, a reference ellipse was used that describes approximately the shape of the orbit for one turn, which is pictured in the following figure.

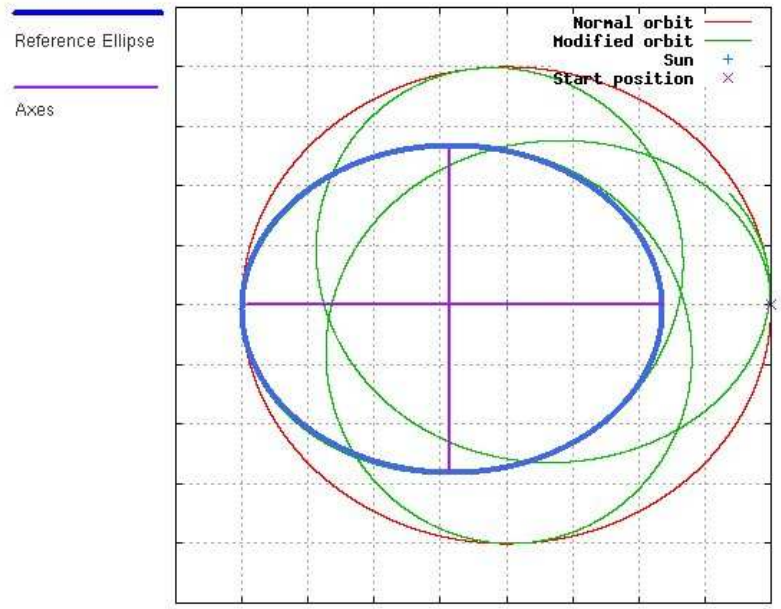

Figure 13: Reference ellipse.

From the qualitative results of the orbit integration one can see that the additional attractive force leads to a turn of the aphelion of the orbit. This aphelion-turn has been investigated more precisely in the following.

Aphelion

To calculate the effective turn in the aphelion the spatial components have been used to calculate the angle of the aphelion with respect to the x-axis. In order to get an overview of the behaviour dependent on the distance from the centre eight initial conditions have been used, as presented in Table 2. Figure 14 shows which angles occured during this investigation.

$GM[\frac{AU^3}{Day^2}]$	$x[AU]$	$y[AU]$	$z[AU]$	$v_x[\frac{AU}{Day}]$	$v_y[\frac{AU}{Day}]$	$v_z[\frac{AU}{Day}]$
0.22e-15	55000	0	0	0	7.34×10^{-5}	0
0.22e-15	50000	0	0	0	7.69×10^{-5}	0
0.22e-15	48000	0	0	0	7.85×10^{-5}	0
0.22e-15	45000	0	0	0	8.11×10^{-5}	0
0.22e-15	40000	0	0	0	8.60×10^{-5}	0
0.22e-15	35000	0	0	0	9.20×10^{-5}	0
0.22e-15	30000	0	0	0	9.93×10^{-5}	0
0.22e-15	28000	0	0	0	1.03×10^{-4}	0
0.22e-15	25000	0	0	0	1.09×10^{-4}	0

Table 2: Initial conditions for the investigation of the aphelion-turn: G is normalized to Solar masses.

From the resulting data it was possible to extract the different angles for the orbits.

$Distance[AU]$	$\frac{d\theta}{dT}[Deg/Day]$
28000	5.06×10^{-08}
30000	5.34×10^{-08}
35000	5.95×10^{-08}
40000	6.45×10^{-08}
45000	6.85×10^{-08}
48000	7.06×10^{-08}
50000	7.18×10^{-08}

Table 3: Aphelion-turn per Day.

It seems to be obvious that the behaviour of θ, the aphelion-angle, follows some kind of function (Figure 14).

Although the behaviour of $\frac{d\theta}{dT}$ seems to follow some kind of function, this function will not be valid for every initial condition. This, one can see from the consideration for some different initial conditions (the three datapoints below the curve) which would lead to elliptical orbits in the case of an usual Keplerian potential and shows that a fitting function cannot be used in general, but depends strongly on the initial conditions.
However, the above results show qualitatively that objects with the initial conditions of a circular orbit, in a potential without the vacuum-energy term, pass to an elliptical one along with a turn of the aphelion, dependent on the initial distance, in a potential including the vacuum-energy.

Eccentricity

Closing this part the change in eccentricty has been considered, in the same way as for the aphelion. It should be noted here again, that the orbital parameters correspond to a model ellipse for one turn of the object (see above). That is because the determination of the eccentricity is not exact, but just an approximation.

In order to determine this parameter the aphelion-distance and the perihelion-

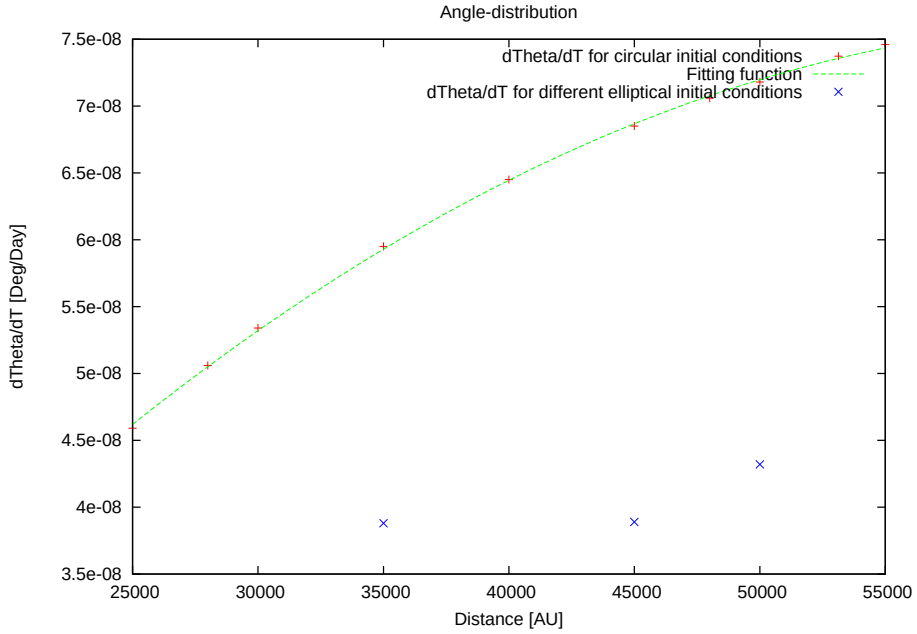

Figure 14: Distance dependent behaviour of the aphelion-turn.

distance of the data has been used. With these values it was possible to calculate the eccentricity via

$$\epsilon = \frac{r_{apo} - r_{peri}}{r_{apo} + r_{peri}}. \tag{23}$$

The values for r_{apo} and the corresponding r_{peri} has been extracted from the data-sets. It should be mentioned that the value for the distance of the pericentre is the smallest distance from the centre. But as one can see from Figure 13, the apocentre and the pericentre do not define the symmetry-axis of the ellipse, because the actual path of the object over one turn is not exactly an ellipse. To describe the path by some kind of orbital parameters this approximating ellipse has been used.

With the above derived values for the apo- and pericentre it was possible to calculate the approximating eccentricites for several initial conditions, which are plotted in Figure 15.

The eccentricities do not not show a clear functional behaviour. The linear fitting function in the figure deviates partially very strongly from the data-points. So it seems that the eccentricities also depend strongly on the initial conditions.

But as in the case for the aphelion-turn, also here one can see that the eccentricity for one turn decreases the smaller the initial distance is. This agrees with the qualitative results that are shown in Figures 3 - 6.

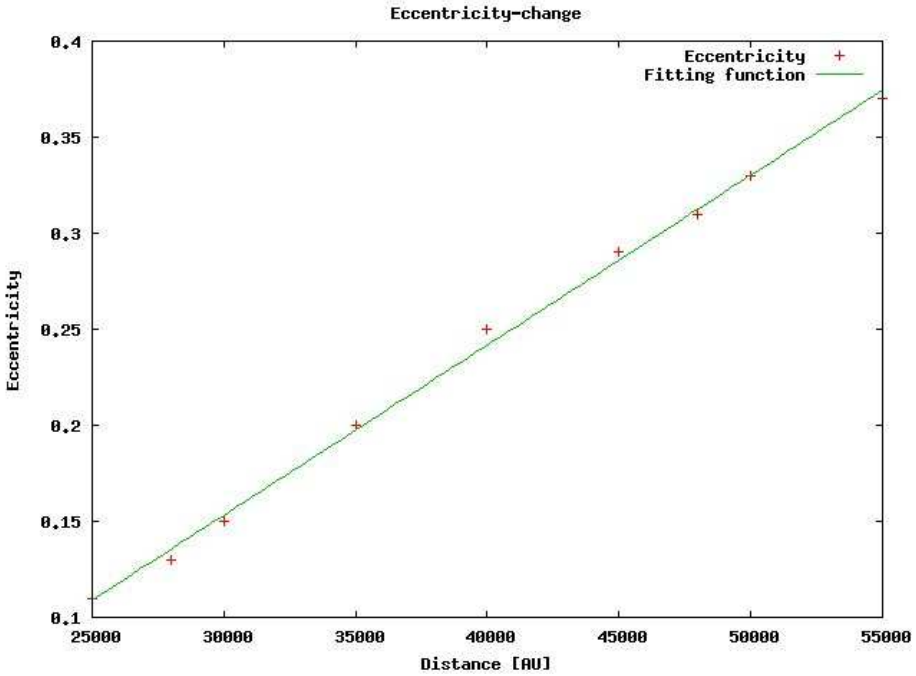

Figure 15: Distance dependent behaviour of the eccentricity.

3.8.3 Error consideration

The used data in this chapter has been calculated via the numercial method of Runge-Kutta. Every numerical calculation contains errors. So also here.
Calculating with Runge-Kutta makes it necessary to define an upper limit for the numerical error. This defined error-limit in the program used for these calculations was of the order of 10^{-16}. This small error-limitation led to the following error-distribution dependent on the distance (Figure 16).

The numerical errors in the distance for different initial conditions are plotted here. At smaller distances the abundance of errors larger than 10^{-22} is quite large. Nevertheless all these errors are very small. The average error is $1.22 \times 10^{-22} \frac{AU}{Day}$ whereas the maximum error is $4.52 \times 10^{-21} \frac{AU}{Day}$. This error in the velocity leads with the chosen time-step-width to an spatial error of the order of $10^{-19} AU$, which is negligible compared to the distances that occur here. Using the usual error propagation for the aphelion-angle and the eccentricity

$$\Delta\theta = \frac{\Delta x y - \Delta y x}{y^2 + x^2}, \tag{24}$$

where x and y are the used coordinates from the data-set to determine the aphelion distance, and

$$\Delta\epsilon = \frac{2(r_{peri}\Delta r_{apo} - r_{apo}\Delta r_{peri})}{(r_{peri} + r_{apo})^2}, \tag{25}$$

the errors for θ and the eccentricities $\Delta\epsilon$ follow to be of the order 10^{-25}. These

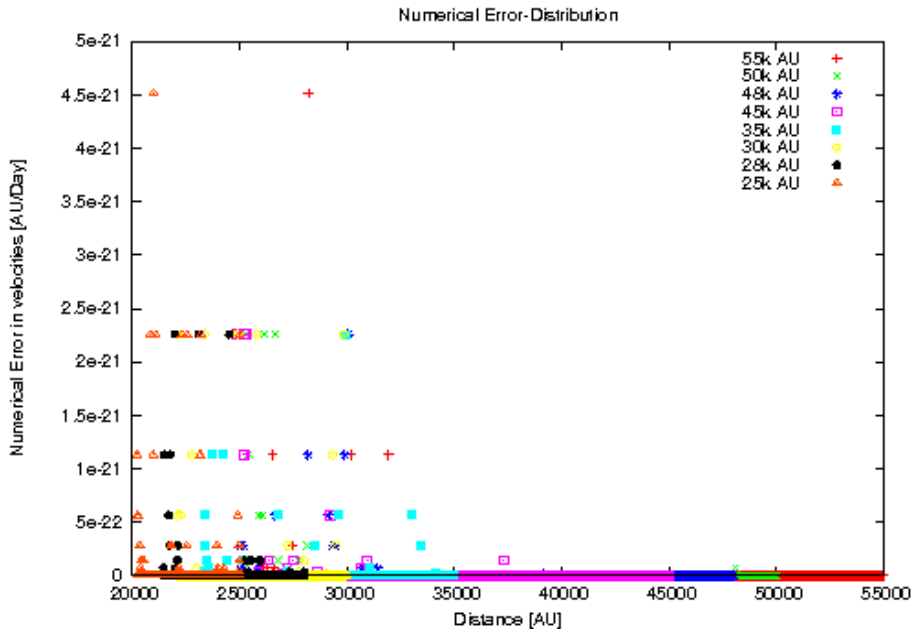

Figure 16: Distance dependent numerical error-distribution

numercial errors are too small to be significant for this discussion.

3.9 Conclusions

This section investigated the influence of a negative time-dependent 'cosmological constant' Λ_- which would lead to an additional attractive force within the Solar System. The additional attraction due to Λ_- causes significant deviations from Keplerian orbits for distances larger than $\sim 20.000 AU$. So objects that would move on cicular orbits in a purely Keplerian potential at such distances would be forced to elliptical orbits going with a perihelion-turn and a change in the eccentricity in a potential compoud of a Keplerian one plus a vacuum-energy contribution.
Considering the resulting spatial and velocity-components from the perspective of an assumed usual Keplerian-potential, these objects would move to very large distances and on orbits with, on the one hand, very high and also very low eccentricities on the other hand.

Although a negative cosmological constant would lead to observable changes in eccentricity, as one can see from the resulting orbits, an object, which moves in the modified field would not be hurled to very larger distances where it would be exposed to the Galactic tidal field and so may leave the Solar System. In contrast it would be bound stronger to the centre due to the additional force.

3.10 Further investigations

As one can see, the simulation of orbits using a negative time-dependent local cosmological constant leads to appreciable results, so further considerations should be made. The investigation shows that for semi-major distances larger than $\sim 20.000AU$ significant deviations from a pure Keplerian orbit appear. Thus Oort cloud objects ought to be affected. This cloud defines the last 'material' border of our Solar System and may feel the influence of the Galactic tidal field. How a negative cosmological constant Λ_- could keep Oort objects away from distortion by the galactical tidal field could be very interesting. It seems that the negative vacuum energy density leads to an additional stability contribution for these objects.

Applying the concept prospected here, to larger scales, e.g. spiral galaxies or dwarf-spheroidals, may also lead to further interesting results. The investigation of how a negative cosmological constant could affect the behaviour of rotation-curves may create a new explanation for the difference between theory an observation.

An important point may also be an inquiry of the behaviour of a time-dependet $\Lambda_\pm$ within a contracting metric (see foregoing chapter).

4 The influence of Modified Newtonian Dynamics (MOND) within the Solar System

4.1 Introduction

Within the framework of stellar dynamics, a modification of the Newtonian dynamics (MOND) has been introduced. Milgrom [10],[11],[12] derived this modification of Newtons second law in order to explain the behaviour of galaxies rotation curves, without using some kind of non-luminous matter (Dark matter).

This modification changes the behaviour of Keplerian objects within the regime of accelerations that are much smaller than a limit-acceleration a_0. This acceleration turns out to be of the order of $10^{-10}\frac{m}{s^2}$ which is, astonishingly, of the same order as the product cH_0 (with c the speed of light, and H_0 Hubbles constant $73\frac{km/s}{MPc}$).

Within the inner Solar System, any influence of this modification on motions of Keplerian objects cannot be expected because the accelerations in this region are much larger than a_0. Nevertheless, in distances of the order of the distance to the Oort cloud the accelerations of bound objects lie within the MONDian regime, excluding external field effects. So it is convenient to investigate how MOND could influence the motions of such objects.

The first part of this section will be a short discussion of the expected results that MOND would cause on orbital motions. The qualitative influence of MOND on Oort objects will be calculated in the second part whereas the discussion of the change of the orbital parameters will be the topic of the third part.

4.2 First considerations

In the run-up to simulations of motions of objects under MONDian influence, some first considerations will be made, in order to get an idea of what one would expect if MOND is taken into account.

4.2.1 Newtons second law

Investigating the distance dependent rotational velocities of stars within galaxies one is faced with an unexpected phenomenon. Using the classical relation between the gravitational force and the centripetalforce

$$\frac{GM}{r^2} = \frac{v_{rot}^2}{r} \Rightarrow v_{rot} = \sqrt{\frac{GM}{r}}, \tag{26}$$

with G Newtons Gravitational constant, M the gravitating mass, r the distance from this mass and v_{rot} the rotation velocity, would lead to decreasing rotation velocities for large distances from the centre. However, this behaviour is not observed.

For large distances the rotation velocities become more or less constant for large radii and so deviate strongly from expectations, which is pictured in Figure 17. There is shown the theoretical rotation curves of a disk-galaxy and a dark halo. The upper curve is the extrapolation of the measured datapoints that represent the actual rotation velocities.

To solve this mystery it seems to be necessary to increase the gravitating mass

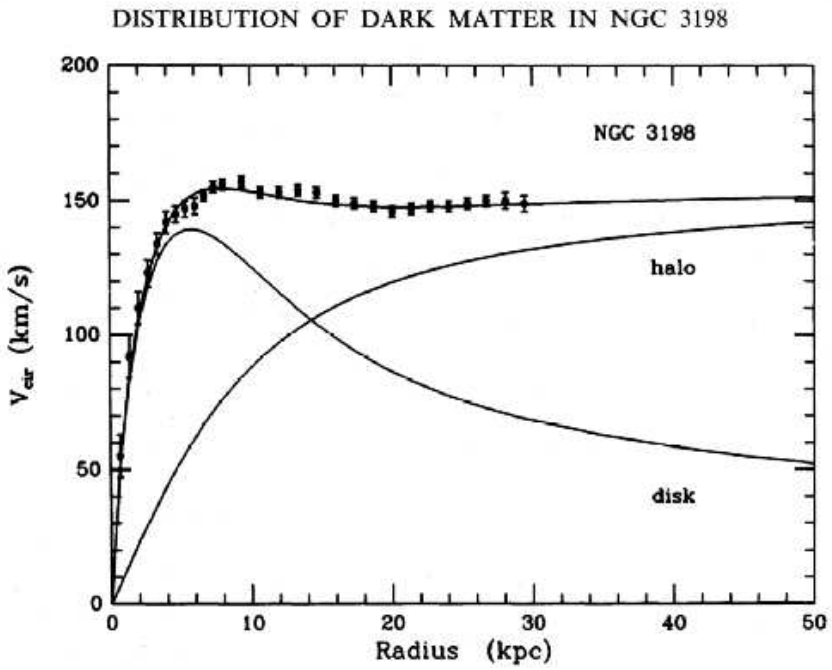

Figure 17: Measured rotation-curve of NGC 3198

around the galaxy. But this mass is not observed and so it must be some kind of non-luminous matter, so called "Dark-matter".
Such a kind of matter seemed to be unrealistic to Mordehai Milgrom. So he developed a formalism to explain the rotation curves of galaxies without any content of Dark Matter.
In this theory Newtons second law

$$F = ma, \tag{27}$$

where F is the acting force, m the inertia mass and a the acceleration, is modified[7]. This modification introduces a limit-accelration a_0 and Newtons second law becomes

$$F = ma\mu\left(\frac{a}{a_0}\right), \tag{28}$$

with the not exactly specified function $\mu(z)$ with the following limit values

$$\mu(z) = \begin{cases} 1 & \text{if} \quad z \gg 1 \\ z & \text{if} \quad z \ll 1 \end{cases} \tag{29}$$

Using this ansatz for small accelerations and keeping $F = \frac{GMm}{r^2} = mg$, where g is the Newtonian acceleration valid leads to

[7]Which led to the notation of **Mo**dified **N**ewtonian **D**ynamics (MOND)

$$ma\mu\left(\frac{a}{a_0}\right) \overset{a\ll a_0}{=} m\frac{a^2}{a_0} = mg_N \tag{30}$$

$$\Rightarrow a = \sqrt{g_N a_0}. \tag{31}$$

The actual acceleration within the MONDian regime ($a \ll a_0$) seems to be $\propto \sqrt{g}$ and not $\propto g$ as in the Newtonian case. So for small accelerations this would lead to larger values than the expected accelerations by Newton.

The larger accelerations increase the rotation velocity of orbiting objects at large distances from the centre, where the MONDian regime is valid. This leads to the observed effect of flat rotation curves for galaxies.

In this work the scales are much smaller than galactic ones. Within the Solar System there are no deviations of planetary motions from expectations observed, so MOND seems not to have any visible effect on these scales.

The value of Milgroms limit-acceleration $a_0 \approx 10^{-10}\frac{m}{s^2}$ seems furthermore to be connected with one of the greatest mysteries in astrophysics, the Pioneer-Anomaly.
This anomaly corresponds to an anomalous acceleration of the Pioneer-crafts towards the Sun with a value of $\approx 8 \times 10^{-10}\frac{m}{s^2}$.
If one considers the distance from the Sun where the gravitational acceleration a is of the same order as a_0 one gets a critical radius of $r_{DM} = 5 \times 10^3$ AU. However the Pioneer-anomaly has been observed at distances between 20 and 70 AU, which is much smaller than distances where MOND would be valid.

Similar to the foregoing chapter one can expect a contribution by MOND at distances that are comparable to the distance of the Oort cloud. At such distances the accelerations should be small enough to see MONDian effects.
The actual accelerations there should be larger than the Newtonian ones and so must lead to deviations from pure circular Keplerian orbits. These deviations may be similar to those of Λ_- which led to elliptical orbits that affect a turn of their aphelion.

4.3 The calculation of MONDian acceleration

In order to get the possibility of a comparsion of MONDian effects and effects due to Λ_- the resulting orbits within the MONDian regime have been calculated in a similar way as for Λ_-.
It has been necessary to include the MONDian acceleration into the used orbit-integrating program (see Appendix).
With the goal of a consistent transition from Newtonian to MONDian regime an expression for $\mu(z)$ has been used which has the following form

$$\mu(z) = \frac{z}{1+z} \tag{32}$$

and shows the demanded behaviour for small accelerations (see above).
Using form (31) the equation of motion becomes

$$\begin{aligned} ma\mu\left(\frac{a}{a_0}\right) &= \frac{GmM}{r^2} = mg_N \\ a\frac{a/a_0}{1+a/a_0} &= g_N \\ a^2 - g_N a - g_N a_0 &= 0 \end{aligned} \tag{33}$$

$$\Rightarrow a = \frac{g_N}{2} + \sqrt{\frac{g_N^2}{4} + g_N a_0}. \tag{34}$$

As done in the framework for Λ_-, any external forces like the gravitational tidal field has been neglected during the calculations.
Using the same set of initial conditions as for Λ_- delivered the orbits of Oort cloud objects that are presented in the following section.

4.3.1 Resulting orbits within the MONDian regime

A modification of Newton's second law in the way shown in the foregoing section excludes the calculation for every individual component, because MOND does not depend on the chosen coordinate-system.
So it was necessary to calculate the acceleration for the absolute distance via equation (34) first and strip it into three spatial components. Doing, this delivers the following deviations from Keplerian orbits (Figures 18 - 21).

Considering these orbits it is obvious that indeed MOND would cause strong deviations from Keplerian orbits. Differently from the results for Λ_- these deviations seem to be strong at distances far below 50.000 AU. This point will be discussed in a later section.

Just as done for the vacuum-influenced orbits, the behaviour of the orbital parameters will be discussed. Also here a distinction between Active and Passive orbital parameters will be made.

4.4 Change of orbital parameters

To investigate the change of the orbital parameters the orbit with the initial distance of 50.000 AU has been used.

4.4.1 Passive orbital parameters

Analogous to the investigation in section 3 the passive orbital parameters could be calculated by the program in a direct way. So these parameters correspond to best fitting orbits within a pure Keplerian potential.

Semi-major-axis and aphelion-distance

To calculate the value of the semi-major-axis a equation (20) has been used

$$a = \frac{r}{2 - rv^2/\mu}. \tag{35}$$

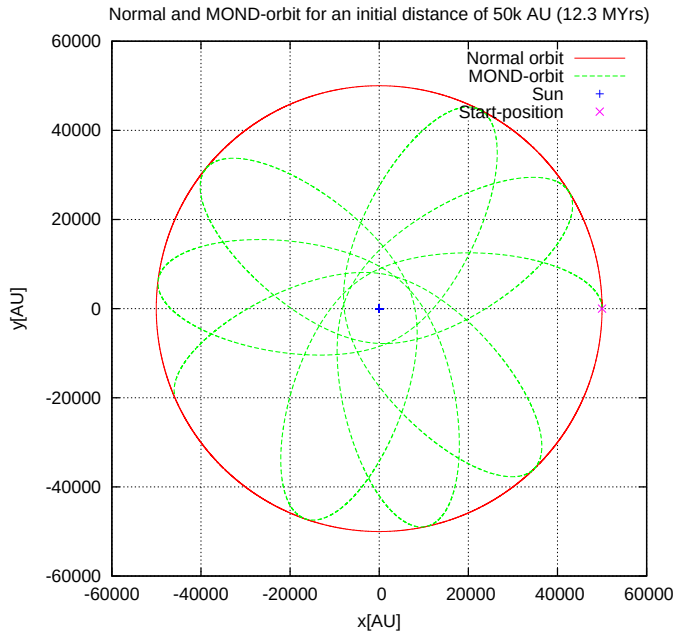

Figure 18: Resulting orbit for an initial distance of 50.000 AU

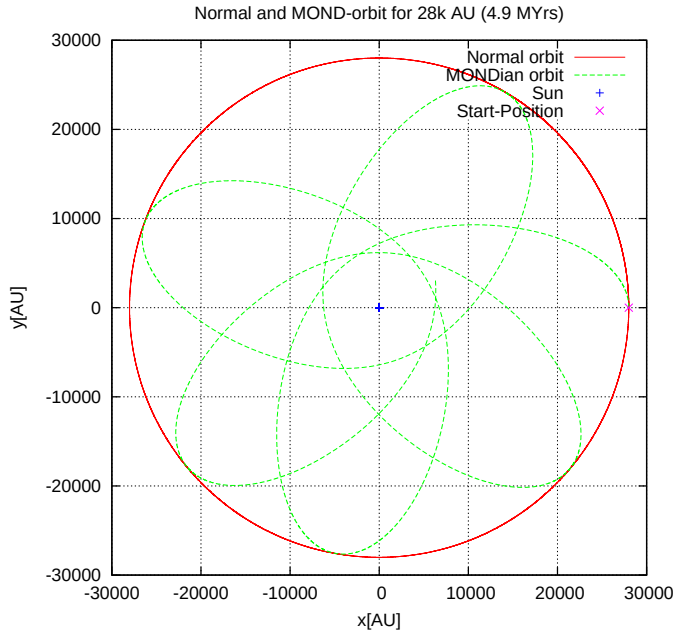

Figure 19: Resulting orbit for an initial distance of 28.000 AU

The result of this calculation is shown in Figure 22.

The behaviour of a that is shown here indicates that the best-fitting orbits

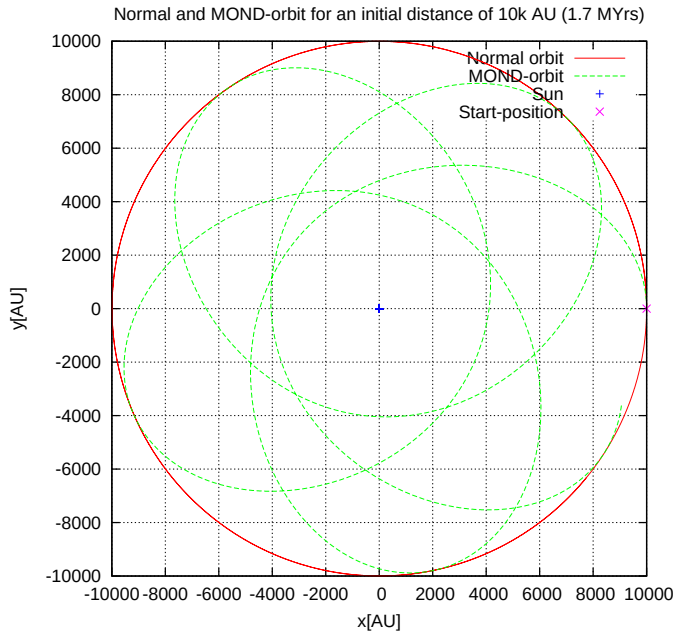

Figure 20: Resulting orbit for an initial distance of 10.000 AU

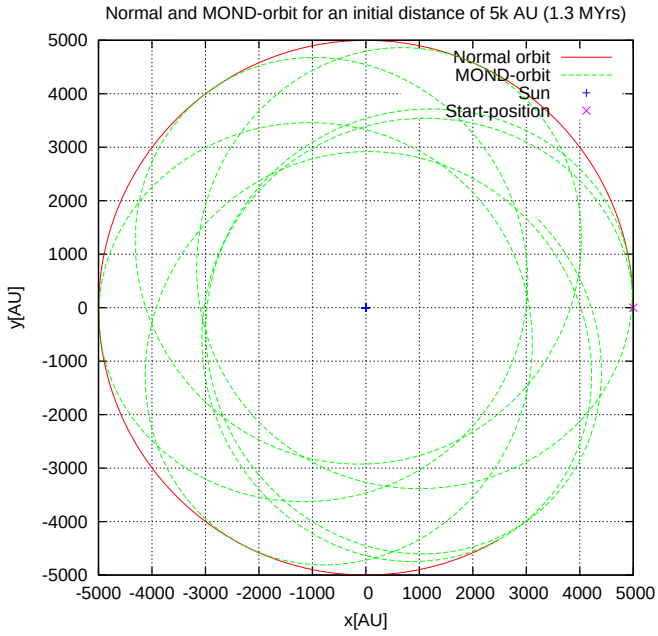

Figure 21: Resulting orbit for an initial distance of 5.000 AU

for an usual Keplerian potential should be mostly hyperbolic. This becomes obvious if one compares the values of a between to peaks (Figure 23).

Prior the first peak that is shown here the value of the semi-major-axis is nega-

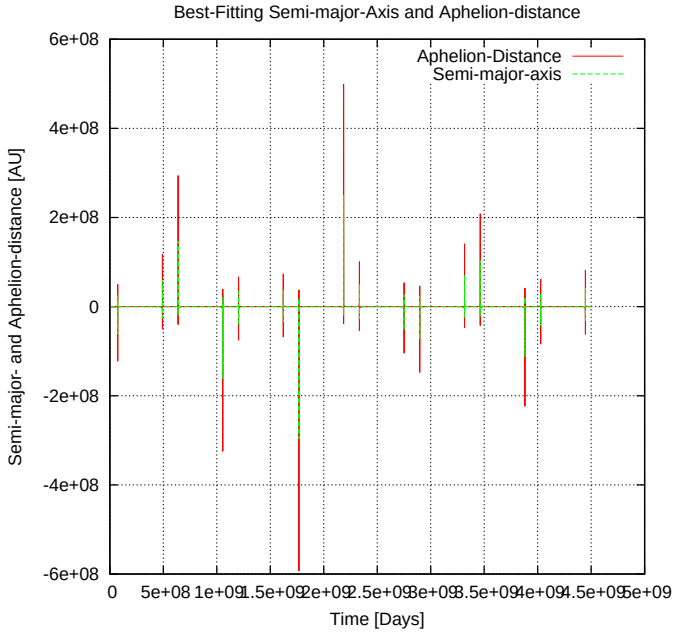

Figure 22: The behaviour of the instantaneous best-fitting semi-major-axis and the aphelion-distance with time

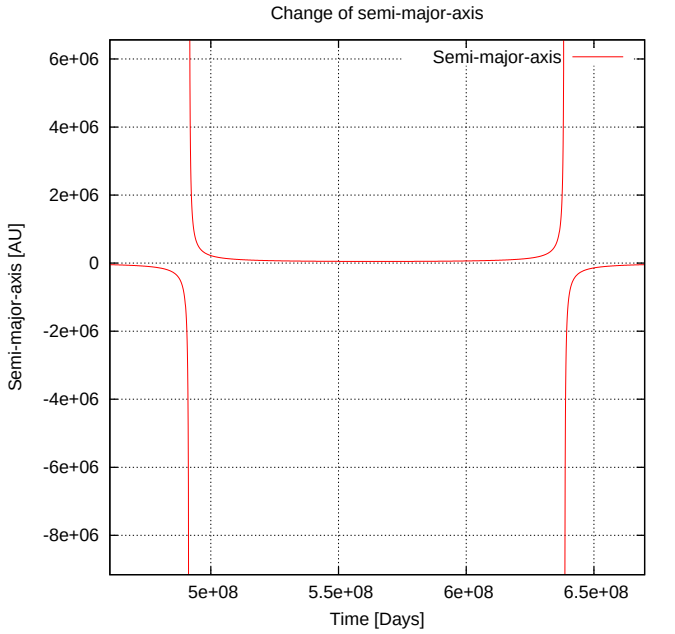

Figure 23: The behaviour of the semi-major-axis between two peaks

tive. An ellipse always has a positive semi-major-axis, but for a hyperbolic orbit its defined negative. So in this region -which correpsonds to a position closely before the object reaches the aphelion-distance under MONDian influence- one would expect to observe hyperbolic pathways for such objects.

Between those two peaks a jumps to positive values that correspond to closed orbits.
As one can see the peaks appear paired equidistantly. Locating these groups on the calculated orbit marks positions before and after the aphelion-passage (Figure 24). So what one would expect to observe for Oort-Objects in such

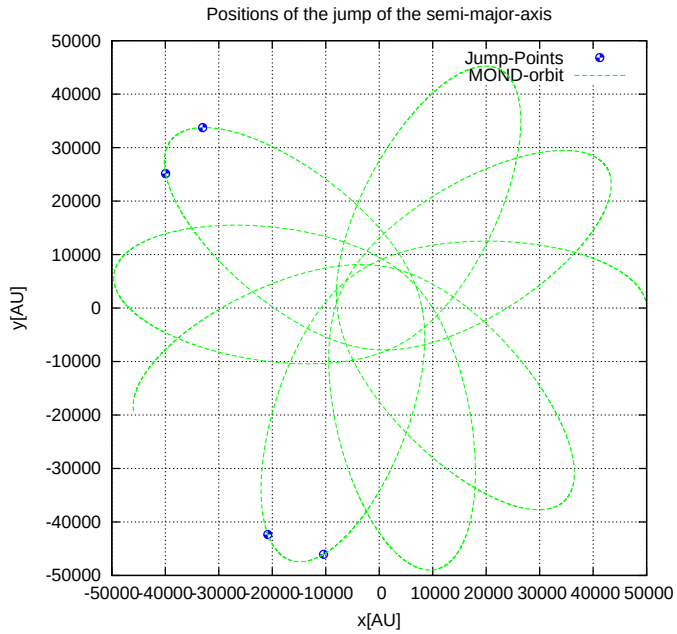

Figure 24: Points on the orbit where the semi-major axis a jumps to the opponent sign

distance are closed elliptical orbits. For the inner regions the behaviour of the orbits would be hyperbolic.
This result can also be confirmed by investigating the best-fitting eccentricities.

Eccentricity

The time where negative values of a would appear seems to be much larger than the time of positive ones. This is obvious from the consideration of the time-distances between the peaks in the developing semi-major-distance. This means that the most of time such test-objects would be observed as objects on hyperbolic orbits.

In order to confirm that behaviour the best-fitting eccentricities has been

calculated according to Λ_- via

$$\epsilon = \sqrt{1 - \frac{p_\phi^2}{a\mu}}, \tag{36}$$

where p_ϕ is again the conserved angular-momentum, a the semi-major-axis, calculated in the foregoing step and $\mu = G_N M_\odot$ the gravitational constant times the solar mass.
The resulting behaviour of the eccentricities is shown in Figure 25.

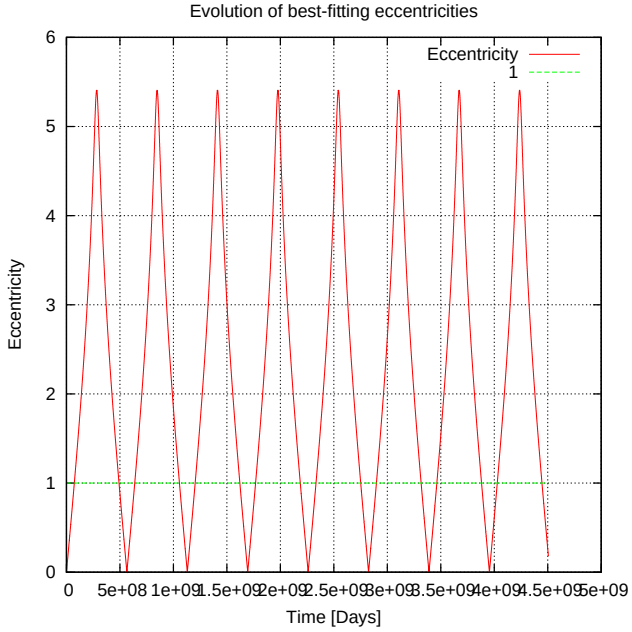

Figure 25: The behaviour of the best-fitting eccentricity

The value of the eccentricity lies between 0 and 6. So one gets eccentricities larger than 1 which correspond to hyperbolic orbits.

The time-comparsion with a^8 validates the above result of comparatively small time intervals with elliptical orbits.

4.4.2 Active orbital parameters

According to the analysis in Section 3, the actual shape of orbits that result from MONDian influence has been investigated. The parameters that describe this shape are called active orbital parameters.

Qualitatively one can say that similar to the orbits under Λ_--influence

[8] Where a is reduced by a factor of 10^{-8}

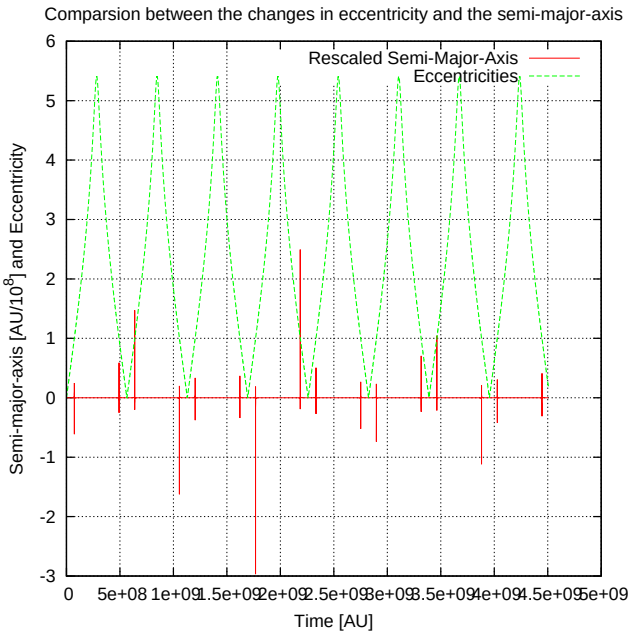

Figure 26: Time comparsion between the eccentricities and semi-major-distances. a is reduced by a factor 10^{-8}. The eccentricities smaller than 1 are located between the two peaks of one pair (see above)

circular Keplerian-orbits are changed into elliptical ones that affect a turn of their aphelion-position. So the two parameters that will be investigated here are the Aphelion-Turn per Day and the approximating eccentricity for one turn.

Aphelion-Turn

Starting with the Aphelion-turn per day $\frac{d\Theta}{dt}$ the angular position of the aphelion has been determined by using again the spatial components of the object. The angle has been compared with the one of the foregoing turn and then divided by the time between these two turns.
Figure 27 shows the behaviour of $\frac{d\Theta}{dt}$ for different initial distances that correspond to cicular orbits in the pure Newtonian case.

Analogous to the Aphelion-turn under the influence of Λ_- it is possible to fit a curve to the data-points.

The blue data points in the plot correspond to elliptical initial conditions. So it seems to be obvious that also here $\frac{d\Theta}{dt}$ does not follow a clear functional behaviour.

Eccentricity

To close this section the dependence of the eccentricity on the initial distance has been investigated.

Just from the qualitative results shown in Figures 18 - 21 one can see that

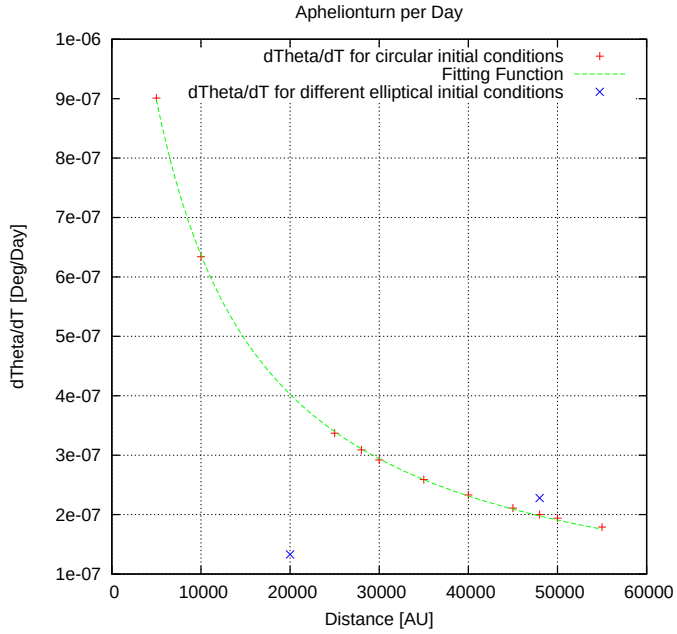

Figure 27: The behaviour of the Aphelion-turn under MONDian influence for circular initial conditions. The blue datapoints correspond to elliptical initial conditions

orbits that correspond to circular ones in Newtonian case, are deformed into elliptical ones with very high eccentricities.
To calculate the eccentricity equation 22 has been used,

$$\epsilon = \frac{r_{apo} - r_{peri}}{r_{apo} + r_{peri}}. \tag{37}$$

Therefore it was necessary to determine the smallest distances to the centre. It should be mentioned here that as in the Λ_--case the smallest distance and the largest one do not define the axis of symmerty of the ellipse. The reason is the perihelion-turn the ellipse affects. So the results presented in the following may not be the exact eccentricities.

The eccentricity increases with the initial distance. This result confirms the qualitative behaviour that is shown in Figures 18 - 21.
For small distances the eccentricity decreases, but seems to be non-zero for distances smaller than $5\times10^3 AU$ which contradicts the above determined critical radius of $r_{crit} \approx 5000 AU$.

4.5 Conclusions

The motion of Oort Cloud objects under MONDian influence causes strong deviations from pure circular Keplerian orbits. The orbits are transformed into elliptical ones affecting an aphelionturn additionally.

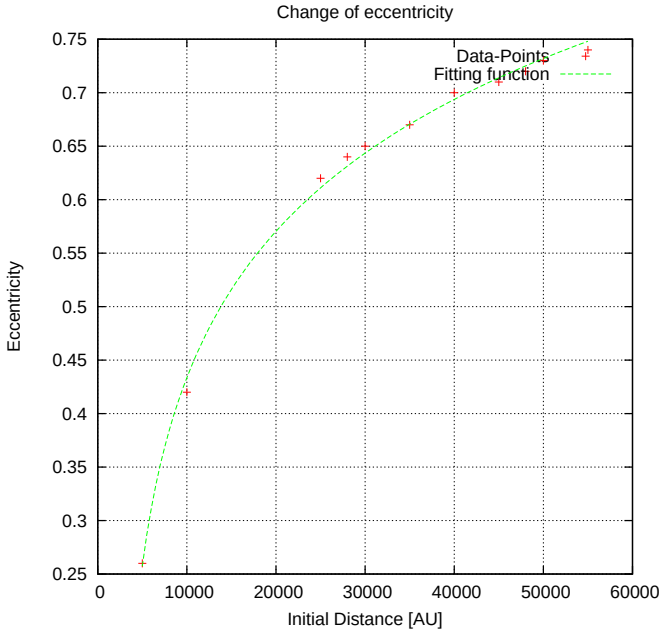

Figure 28: The change of eccentricity for several initial distances

Astonishingly there still remain strong deviations at a distance of $5000AU$ which defines the distances from the central mass where the Newtonian acceleration and a_0 are equal. The reason for this could be that this radius lies within the transition range from pure Newtonian to MONDian regime. There is not a sudden transition between these two regimes. Contrary it has to hold

$$a \ll a_a \tag{38}$$

where a is the actual acceleration.
The used equation to describe this transition (equation (33)) is neither pure Newtonian nor MONDian and so one could expect mixed effects at distances between these two regimes.

5 The influence of suggestive Dark-Matter Halo

The third possible source of a perturbation of the usual Keplerian potential is a suggestvie halo of Dark-Mark bound to the Solar-System. There are several possibilities how such a halo could look like.
In this thesis the mass-density profile will decreace with $\propto \frac{1}{r}$.
In the first part the motivation of this profile will be discussed. In order to keep planetary motions unperturbed a value for the mass of the DM-halo will be determined in the second part. The third part will be the computation and investigation of the influence such a halo would have on Oort-cloud objects.

5.1 Dark-Matter density profile within in the Solar System

One of the most mystirious phenomena in astronomy is the above mentioned Pioneer-Anomaly.
In order to explain this mystery the idea appeared that a suggestive Solar System Dark-Matter halo could cause the deviations in the acceleration that are observed.

This anomolous acceleration of the order of $10^{-10}\frac{m}{s^2}$ seems to stay constant at least over heliocentric distances between $20 - 70AU$.
If some kind of a DM-halo bound to the Solar System, causes this phenomenon it must show a special mass-density-profile. How this profile could look like will be derived in the following.

Lets assume a mass-density-profile of the form

$$\rho_{DM}(r) = \rho_0 r^n \tag{39}$$

with ρ_0 beeing the density in a distance of $r_0 = 1AU$, r the distance and n in the first instance a real number.
Using the Poisson-equation one can derive the corresponding potential for this profile.
Assuming spherical symmetry the Poisson-equation can be written as

$$\frac{1}{r^2}\frac{d}{dr}\left(r^2\frac{d}{dr}\Phi_{DM}\right) = -4\pi G\rho_{DM} \tag{40}$$

with Φ_{DM} being the corresponding potential to ρ_{DM} and G Newtons gravitational constant.
Doing some mathematical transitions the potential turns out to be

$$\begin{aligned}
\frac{1}{r^2}\frac{d}{dr}\left(r^2\frac{d}{dr}\Phi_{DM}\right) &= -4\pi G\rho_0 r^n \\
\frac{d}{dr}\left(r^2\frac{d}{dr}\Phi_{DM}\right) &= -4\pi G\rho_0 r^{n+2} \\
r^2\frac{d}{dr}\Phi_{DM} &= -4\pi G\frac{\rho_0 r^{n+3}}{n+3} + C_1 \\
\frac{d}{dr}\Phi_{DM} &= -4\pi G\frac{\rho_0 r^{n+1}}{n+3} + \frac{C_1}{r^2} \qquad (41) \\
\Phi_{DM} &= -4\pi G\frac{\rho_0 r^{n+2}}{(n+3)(n+2)} - \frac{C_1}{r} + C_2 \qquad (42)
\end{aligned}$$

With the well known relation $F = - \bigtriangledown \Phi$ the gravitational force due to the above density-profile is

$$F_{DM} = -4\pi G \frac{\rho_0 r^{n+1}}{n+3} - \frac{C_1}{r} \tag{43}$$

In order to get a force that does not depend on the distance r, n has to be chosen equal to -1 and the integration-constants $C_1 = C_2 = 0$. Then the density-profile for the suggestive Dark-Matter-Halo is given by

$$\rho(r) = \frac{r_0 \rho_0}{r} \tag{44}$$

This kind of density-profile corresponds to the one given by Anderson et. al. [15].

5.2 Dark-Matter Halo mass

The question remains: Which mass the above DM-halo has to have in order to keep the planetary ephemeries unpersuaded? To answer this question the change of the planetary ephemeries, caused by different halo-masses, has been investigated.
Every additional gravitational force or modification of gravity has to reproduce the existing orbital parameters of the outer planets. With this criterion the orbit of Uranus that moves in distances between 18 - 20 AU has been integrated under the influence of distinct halo-masses and then compared with the pure Keplerian orbit.
The halo-mass can be fixed by choosing ρ_0 respectively and has been determined in a distance of 50 AU[9]. Figure 29 shows the deviations in distance r for five different halo-masses.

It turned out that a halo-mass in such a distance has to be of the order of $10^{-4} M_\odot$ (corresponding to the green dashed line) in order to cause an acceleration like the one of the Pioneer-anomaly.
Such an acceleration would cause strong deviations of Uranus' orbit that have not been observed until today. Because of this the halo-mass has been chosen to be of the order of $10^{-6} M_\odot$ as an upper limit with a corresponding $\rho_0 = 1.27 \times 10^{20} \frac{kg}{m^3}$. Such a mass would cause deviations of the order of 10^{-5} in the orbit of Uranus and is in good accordance with the estimation of Anderson et. al.

The constant acceleration due to the DM-halo with a density-profile $\sim \frac{1}{r}$ is then given by

$$a_{DM} = 2\pi G \rho_0 \simeq 1.18^{-13} \frac{AU}{Day^2} = 2.37 \times 10^{-12} \frac{m}{sec^2} \tag{45}$$

[9] According to Anderson et. al.

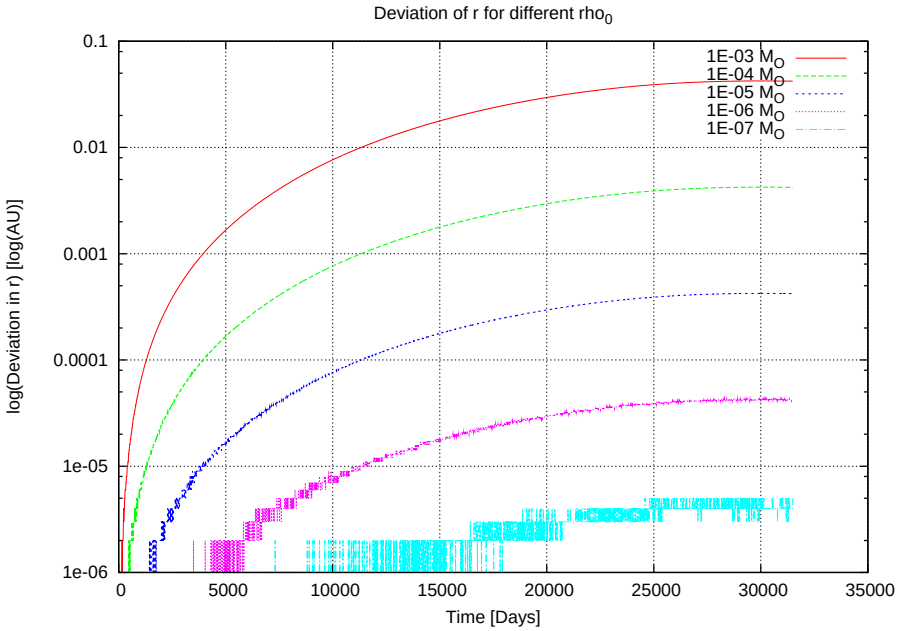

Figure 29: Deviation in distance r for different halo-masses

5.3 Resulting orbits with a Dark-Matter Halo

Using the derived DM-density profile, the deviations of orbits from the pure Keplerian case has been calculated with the orbit-integrating programme. The initial conditions were the same as for Λ_{-} and the MONDian case. The results are shown in Figures 30 - 33.

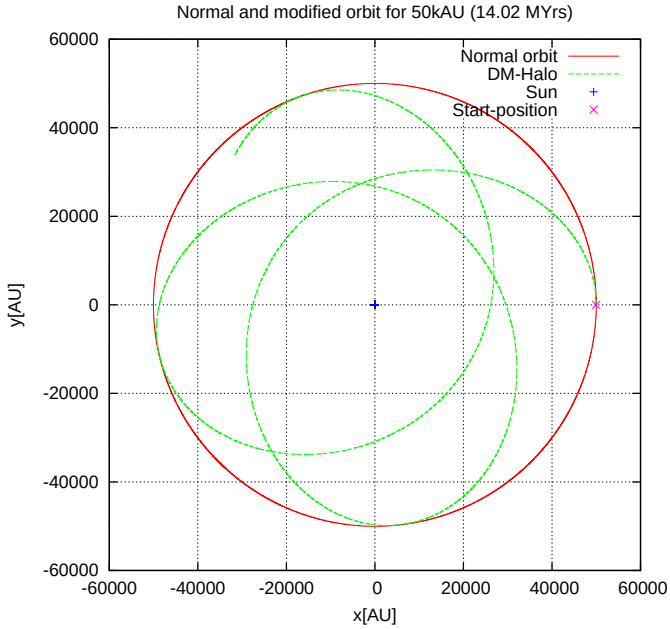

Figure 30: Resulting orbit for an initial distance of 50.000 AU

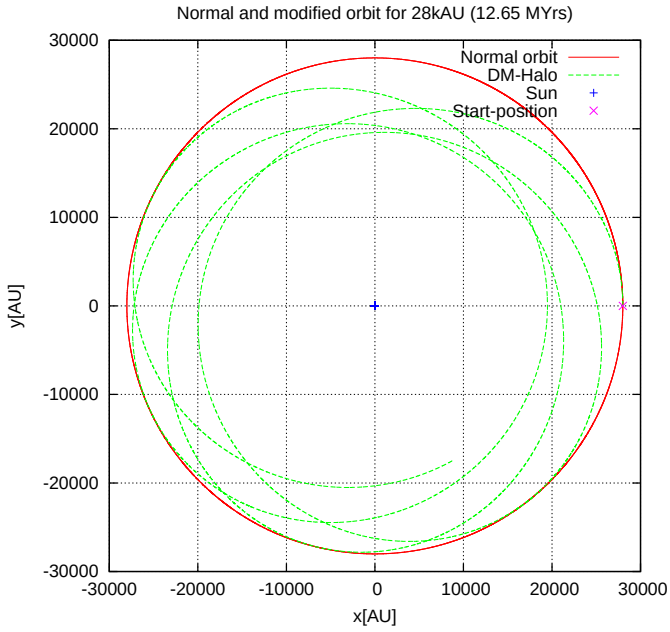

Figure 31: Resulting orbit for an initial distance of 28.000 AU

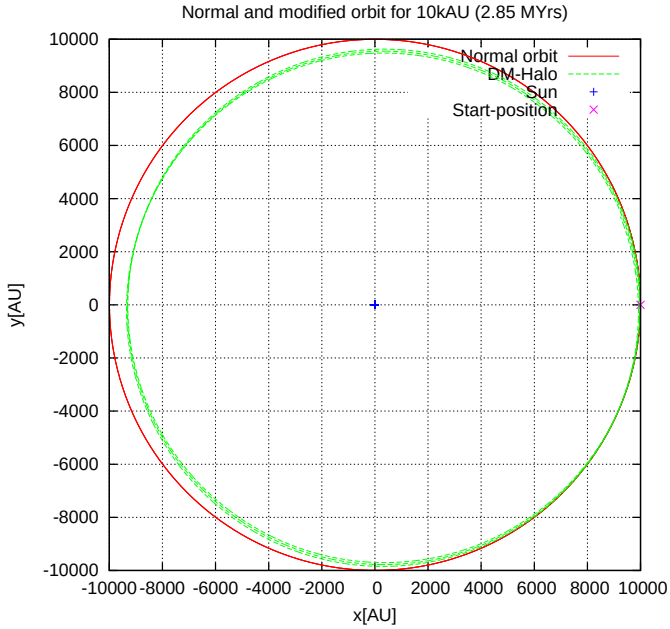

Figure 32: Resulting orbit for an initial distance of 10.000 AU

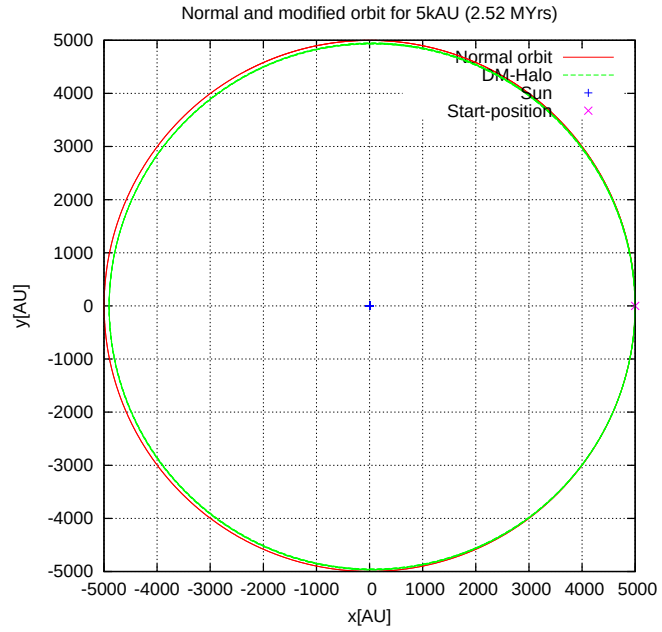

Figure 33: Resulting orbit for an initial distance of 5.000 AU

As in the cases for Λ_- and MOND objects on a Newtonian circular orbit are forced to elliptical ones affecting an aphelion-turn. In distances of the order $10^3 - 10^4 AU$ the gravitational acceleration due to the central mass is small but

is almost equal to the constant acceleration due to the DM-halo.
To get further information about the deviations the active and passive orbital parameters will be considered in the next section.

5.4 Change of orbital parameters

5.4.1 Passive orbital parameters

Accordingly to the analysis of the orbital parameters for the motions under Λ_- and MONDian influence the parameters of the orbits under the influence of a DM-halo has been investigated. The results are presented in this and the next section.

Semi-major-axis and aphelion-distance

As well as done for the first two cases the semi-major-axis for every time step has been calculated with equation (20). This delivered the following evolution of these parameters. The semi-major-distance is always positive. So a DM-halo

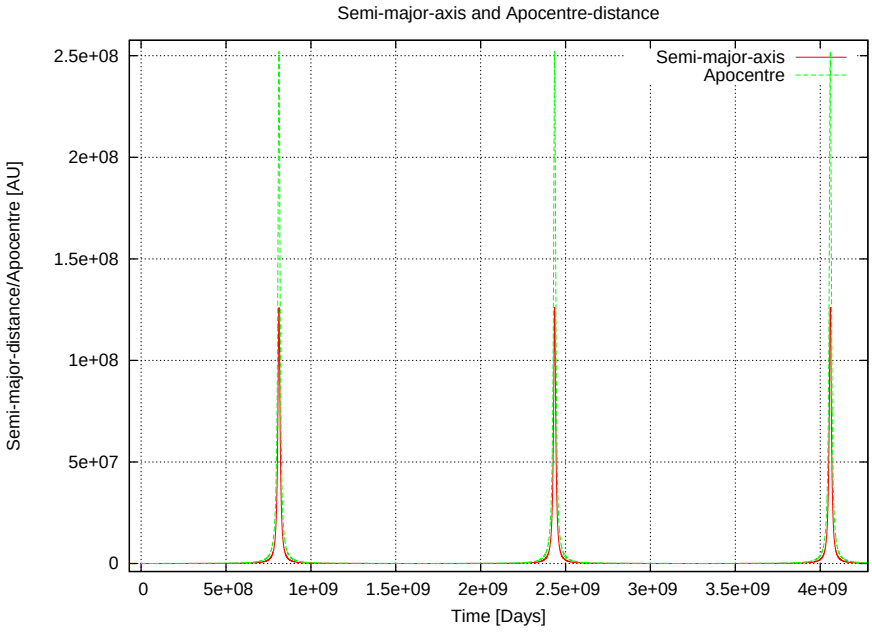

Figure 34: Semi-major-axis and aphelion-distance under DM-influence

would only cause spatial and velocity components that would lead to closed orbits in Keplerian case. This result is confirmed by the time-evolution of the passive eccentricity.

Eccentricity

The eccentricity is always smaller than 1 which corresponds to closed Kep-

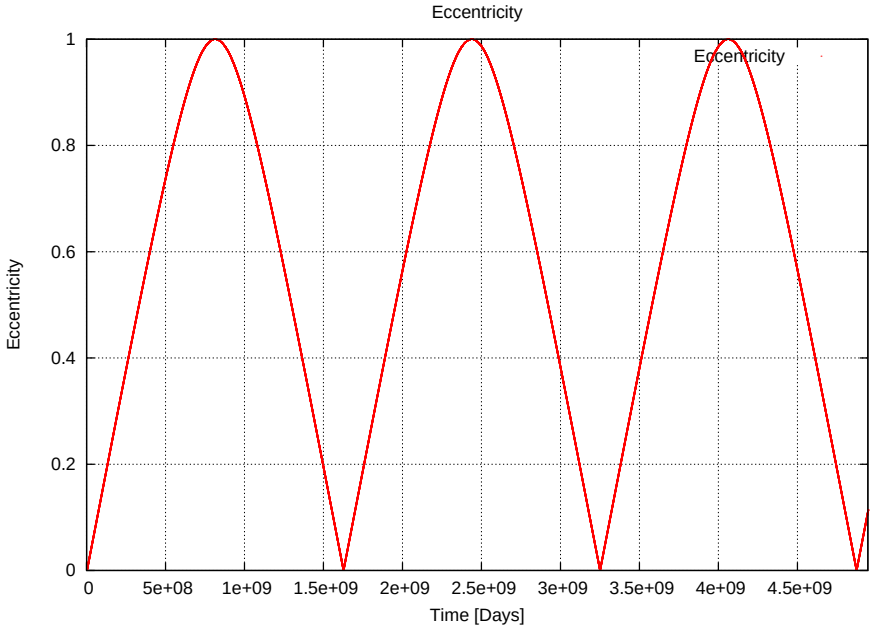

Figure 35: Eccentricity-evolution under DM-influence

lerian orbits. A hyperbolic or parobolic orbit would have an eccentricity > 1[10].

5.4.2 Active orbital parameters

The active orbital parameters has also been determined in the same way as for the other two modifications. They describe the actual shape of test particles orbit.
It should be mentioned that the obvious functional behaviour of these parameters depend strongly on the initial conditions. The parameters appearing in this thesis belong only to circular initial conditions. For high or low elliptical orbits they would be completely different.

Aphelion-Turn

Figure 36 shows the behaviour of the aphelion-turn per day for different initial distances R. From this figure it is obvious that for large initial distances the DM-halo causes high angle turns in the resulting orbits.
The qualitative results in Figures 30 - 33 show that the circular orbits also are changed into elliptical ones.

Eccentricity

The eccentricities of the orbits for different initial conditions are plotted in Figure 37. They seem to change lineary accordingly to the case of Λ_-.

[10] Compare MONDian case

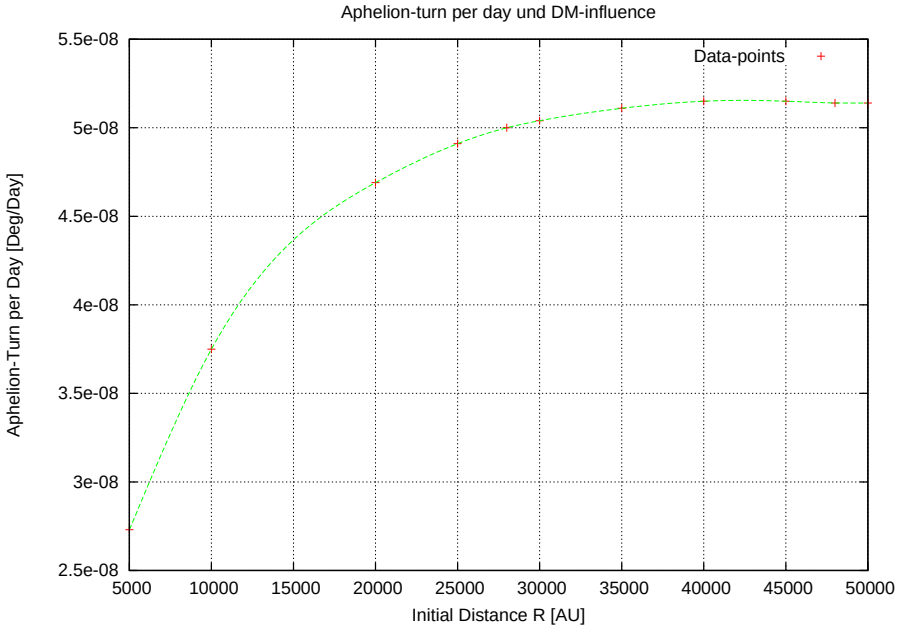

Figure 36: Aphelion turn under DM-influence

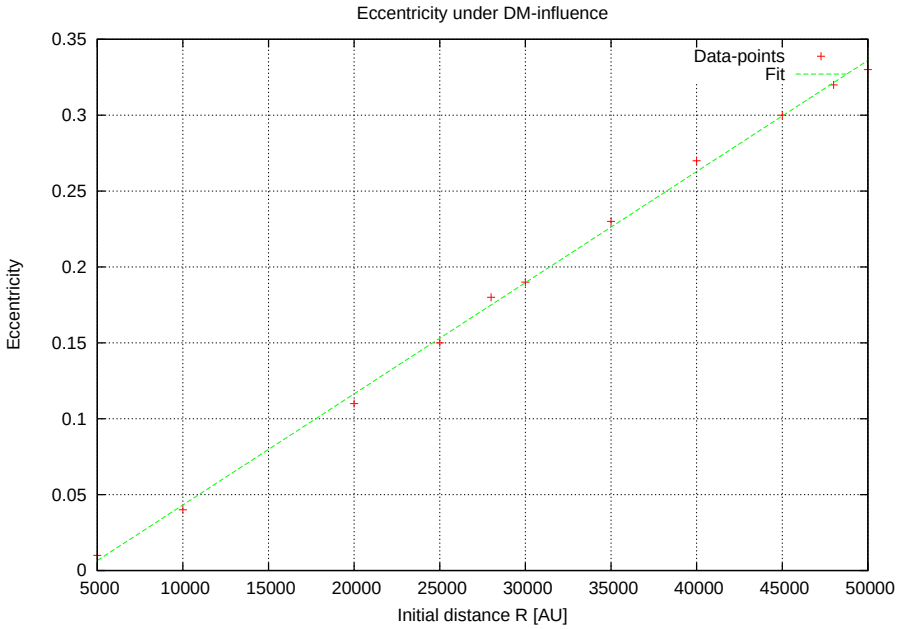

Figure 37: Eccentricities under DM-influence

5.5 Conclusions

In this section the influence of a Dark-matter halo with a density profile which goes with $\frac{1}{r}$ has been investigated. Such a profile causes a constant acceleration towards the centre that changes circular Keplerian orbits with initial distance between $5000 - 50000AU$ into elliptical ones, affecting an aphelion-turn additionally. The results of this investigation are highly comparable to those of Λ_{-}. As in that case the orbits of the test-particles deviate strongly from the pure Keplerian case but still deliver spatial and velocity compontens that correspond to closed Keplerian orbits.

6 Comparsion of the three modifications of gravity

Every modification of gravity considered in this thesis caused strong deviations from pure Keplerian orbits. In this section these deviations will be compared.

6.1 Relative Acclerations

To distingush between the strength of the different cases of modification the additional acceleration in a distance of $50000AU$[11] has been calculated.

Case	Acceleration $\frac{AU}{Day^2}$	$100\frac{a_{Newton}}{a_{mod}}[percent]$
Newtonian	1.18E-13	100.00
Λ_-	1.55E-13	76.58
MOND	1.21E-12	9.82
DM-halo	1.18E-13	100.00

Table 4: Acceleration-Comparsion

As one can see the Λ_-- and DM-acceleration are of the same order of magnitute as the Newtonian one at that distance. The acceleration due to the MONDian effect seems to be larger about one order an delivers a first difference to the other modifications.
To get an overview of the distribution of the accelerations Figure 38 shows the relative contributions to the Central-Mass-Newtonian accleration.

For small distances the contribution of Λ_- and DM ist quite small and negligible. But the MOND-induced acceleration is always larger than the pure Newtonian one, even for distances near the critical radius $r_{MOND} \simeq 5000AU$.

6.2 Qualitative comparsion

The additional accelerations resulting from the three modifications increased the pure Newtionan acceleration. So it has been expected that the test-particle should near the central mass instead of staying on orbits with constant radius. This behaviour could be observed in all three cases. Also a turn in aphelion has been caused under the different modifications.
The results from Λ_-- and DM-case seem to be very equal. At large radii the deformation of the orbit is large and almost negligible at distances of about $5000AU$. In the MONDian case there are still strong deviations from Keplerian orbit even at such small distances.

6.3 Comparsion of the passive orbital parameters

In order to get information of how one would observe an object under the influence of some gravitational modification under the assumption of a pure Keplerian case, the orbital parameters for every component have been calculated. Figure 39 shows a comparsion between the semi-major-axes dependent on time.

[11] The analysis of the passive orbital parameters was done for that distance

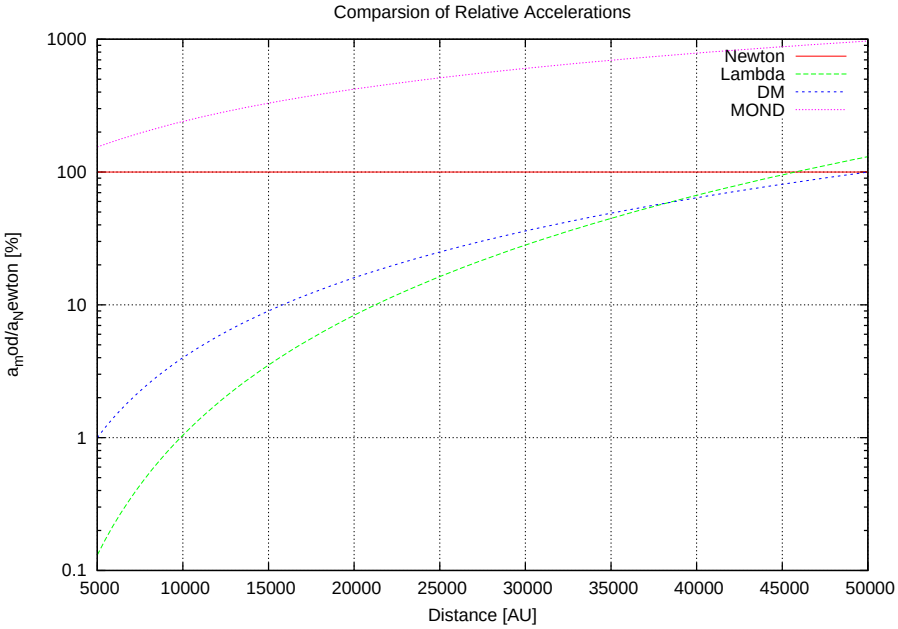

Figure 38: Relative contribution to the central-mass acceleration

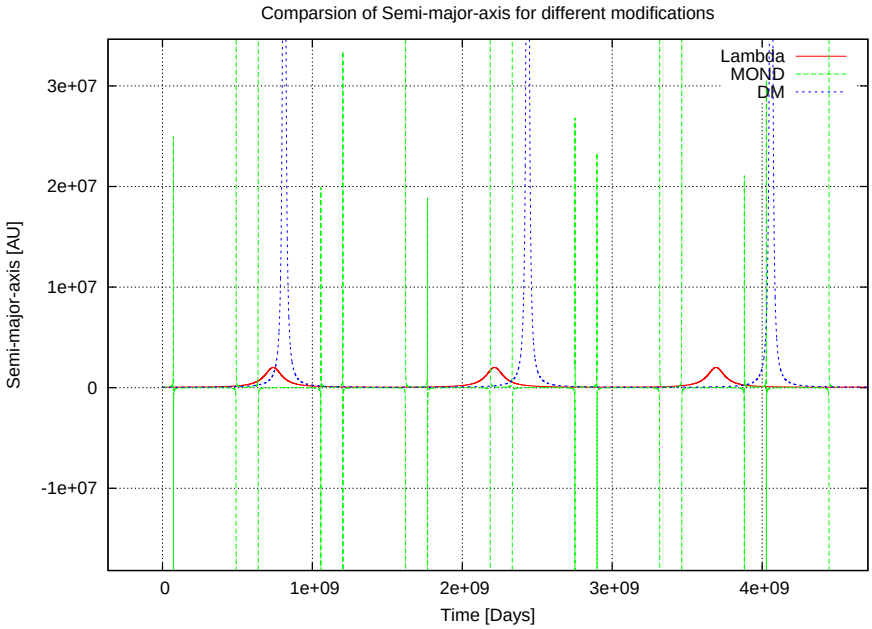

Figure 39: Comparsion between the Semi-major-axes

This orbital-parameter tells alot about the kind of the orbit one would observe. The behaviour of the semi-major-distance for Λ_- and a Dark-Matter-halo seem not to be correlated with each other. For the DM-halo the object would be able to reach much larger distances as in the Λ_--case. However, objects with such kind of semi-major-axis would be still bound to the central mass. This does not hold for MOND. Here one can see very clearly that the value for the semi-major-axis a also reaches negative values that are only defined for hyperbolic orbits. So MOND would mainly cause orbits that would be hyperbolic in pure Keplerian case.
The large difference between the values for a for Λ_- and DM can be explained by the contribution to the Newtonian forces due to the central mass on the one hand and by the fact that in the DM-case the object always feels a constant acceleration whereas the contribution from the negative cosmological 'constant' decreases with decreasing distance.

6.4 Comparsion of the active orbital parameters

The active orbital parameters have been introduced to describe the actual shape of influenced orbits. As shown in section 6.2 all three considered modifications cause in general the same deviations from Keplerian circular orbits. The differences are the Aphelion-turn per day $\frac{d\Theta}{dt}$ and the real eccentricities for one turn. A comparsion between $\frac{d\Theta}{dt}$ for every modification is shown in Figure 40.

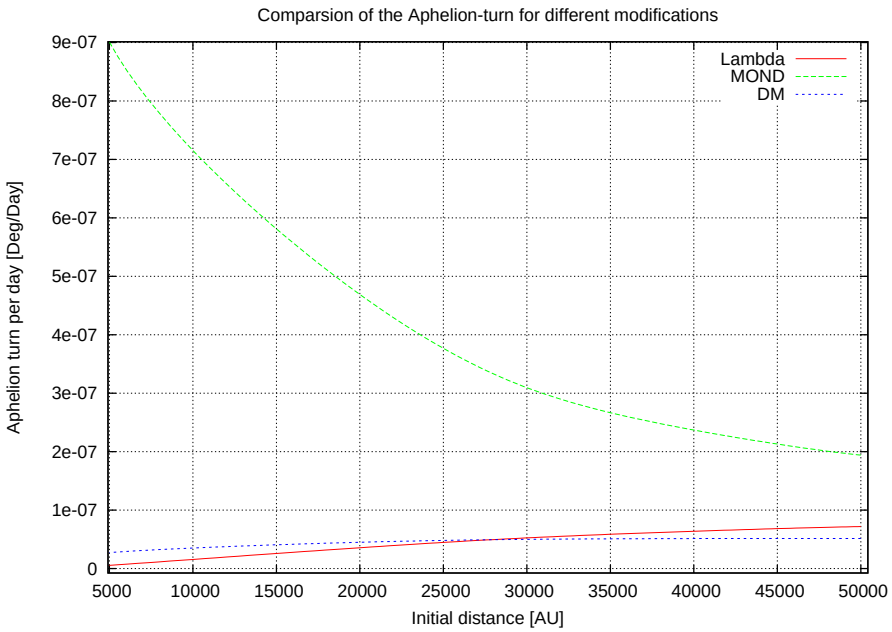

Figure 40: Comparsion between the Aphelion-turns per day

It is very conspicuous that this orbital-parameter is quite similar for Λ_- and Dark Matter. Both decrease slightly for large initial distances and become small for small distances. In the MONDian case this behaviour cannot be observed.

Contrary for small distance $\frac{d\Theta}{dt}$ increases strongly and decreases for large distances. This behaviour could be explained by considering equation (33). For large distance the effective acceleration becomes $\approx \sqrt{g_N a_0}$ and for distances about $5000AU$ this value is larger than for $50000AU$. This is one of the most important differences between MOND and the other two modifications:

The Newtonian acceleration due to the central mass and the MONDian acceleration a_0 are not linearly. From this it is obvious that one would expect a complete different behaviour for the eccentricities for MOND and the other two cases. Figure 41 shows quite well that this difference exists.
While the eccentricities of Λ_- and DM seem to run similary, MOND causes a completly different range for the eccentricity.

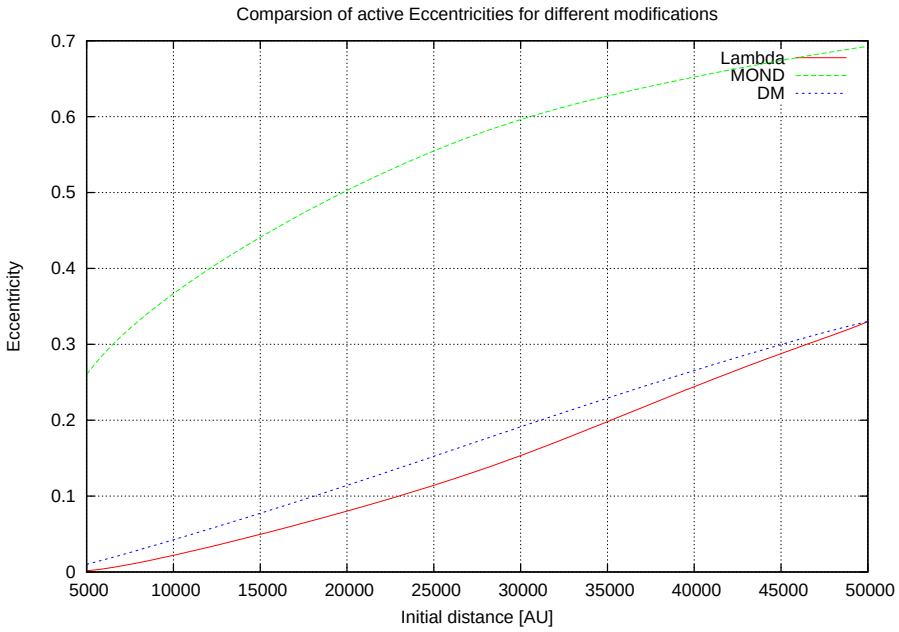

Figure 41: Comparsion between the eccentricities

7 Summary

In this thesis the influence of three modifications of gravity has been investigated. The first one was a negative time-dependent cosmological "constant" Λ_- that causes an additional attraction towards the centre of the considered system.
The second modification was a one in Newtons second law $F = ma$ called MOND. This modification has been developed in order to find an alternative to some kind of hidden mass, called Dark-matter which was the third considered modification.
The used Dark-matter-halo had a special density profile $\sim \frac{1}{r}$ that generates a constant acceleration towards the centre, according to the Pioneer-acceleration.
All the modifications caused strong deviations from Keplerian circular orbits. The orbits have been transformed into elliptical ones affecting an aphelion-turn additionally.

The analysis of the passive and active orbital parameters has shown strong differences between MOND on the one side and Λ_- and Dark-Matter on the other one. The MONDian effect seems to dominate even for small distances of about $5000AU$ whereas the other two modifications vanish at such distances. An explanation for this difference can be found in the non-linearity of MOND and the fact that the contribution to the pure Newtonian acceleration is quite larger than for Λ_- or DM.
However, every considered modification of gravity would cause effects that should be observable. An idea of how these effects could be verified or disproved will be discussed in the next and last section of this thesis.

8 Further investigations and outlook

Every modification of gravity has been considered at large distance of about $5000 - 50000AU$ and seems to be negligible on scales of the inner Solar System. A direct observation at distances of the order of the Oort cloud seems to be completly excluded because every observation is limited by the possible resolution of the used telescope and furthermore by the observation time that would be necessary to recognize any deviation from the pure central mass Newtonian case at such large distances.
Another possibility than the direct observation of long periodic Oort cloud objects could be some kind of experiment on an Earths satellite placed at one of the Lagrangean points.
These points are quasi-stable points within the framework of the Three-Body-Problem where the net gravitational force of the bodies is almost zero. It is for this reason why these points would be appropriate to test at least two of the discussed modifications: Λ_- and a Dark-Matter halo.
To test MOND these points would not be incapable because the external galactic field which has been neglected in this thesis is much larger than a_0 over the whole Solar System and so would not lead to any MONDian effects over the Solar System.
Investigating the additional forces acting on an object at those points and comparing them with the forces due to Λ_- or DM would be a possible test of modified gravity. In addition other modifications could be tested with such an experiment.

Whatever the investigation and development of modified gravitational theories will create, it seems to be obvious that the pure Newtonian Gravity due to central masses is not the whole story.

List of Figures

List of Tables

9 References

[1] Fahr, H.J.; Siewert, M: Imprints from the global cosmological expansion to the local spacetime dynamics (2007)

[2] Fahr, H.J.; Siewert, M: Kinetic study of the ion passage over the solar wind termination shock (2006b)

[3] Cooperstock, F.I.; Faraoini; V.; Vollick, D.N.: The influence of the cosmological expansion on local systems (1998)

[4] Carrera, M; Giulini, D: On the influence of the global cosmological expansion on the local dynamics in the Solar System (2006)

[5] Harrison, E.R.: Cosmology: the Science of the universe (1988)

[6] Westermann, S: Der Einfluss der Vakuumenergie auf Bahnen von Keplerobjekten in Zentralkraftfeldern (2004)

[7] Fahr, H.J.: The Cosmology of Empty Space: How heavy is the Vacuum? What We Know Enforces Our Beliefs

[8] Fahr, H.J.; Heyl, M.: Cosmic vacuum energy decay and creation of cosmic matter

[9] Fahr, H.J.; Scherer, K.: The adapted solar wind system as cause for a momentum transfer to the Sun and its consequences for the orbital motions of Keplerian orbits

[10] Milgrom, M.: A modification of the Newtonian Dynamics as a possible alternative to the hidden mass hyptothesis (1983a)

[11] Milgrom, M.: A modification of the Newtonian Dynamics: Implications for galaxies (1983b)

[12] Milgrom, M.: A modification of the Newtonian Dynamics: Implications for galaxy systems (1983c)

[13] Sanders, R.H., McGaugh, S.S.: Modified Newtonian Dynamics as an alternatvie to Dark Matter (2002)

[14] Anderson, J. D.; Laing, P. A.; Lau, E. L.; Liu, A. S.; Nieto, M. M.; Turyshev, S. G.: Study of the anomalous acceleration of Pioneer 10 and 11 (2005)

[15] Anderson, J. D.; Laing, P. A.; Lau, E. L.; Liu, A. S.; Nieto, M. M.; Turyshev, S. G.: Indication, from Pioneer 10/11, Galileo, and Ulysses Data, of Apparent Anomalous, Weak, Long-Range Acceleration (1998)

10 Acknowledgment

11 Appendix

The following shows a short extract from the source-code of the orbit integrating programme designed by Michael Marks and Jan Pflamm-Altenburg.
The programme used a Runge-Kutta method of fourth order to integrate the motions under gravitational influence. To take the modifications into account the originally code had to be changed.
In the original form the accelerations have been calculated directly for every component seperately.

```
int get_acceleration(unsigned int n,double *m,double **r,double **a){
  unsigned int i,j;
  double dr[3],r2,r1,r3,ddr[3]; /* Helpvariables */

 for(i=0;i<n;i++)
    for(j=0;j<3;j++)
      a[i][j] = 0;

  for(i=0;i<(n-1);i++)
    for(j=i+1;j<n;j++){

      /* Distance between object i and j */

      dr[0] = r[j][0]-r[i][0];
      dr[1] = r[j][1]-r[i][1];
      dr[2] = r[j][2]-r[i][2];
      ddr[0] = dr[0];
      ddr[1] = dr[1];
      ddr[2] = dr[2];

      r2 = dr[0]*dr[0]+dr[1]*dr[1]+dr[2]*dr[2];
      r1 = sqrt(r2);
      r3 = r2*r1;
      dr[0] /= r3;
      dr[1] /= r3;
      dr[2] /= r3;

      /* a=G*M/r^2 */

      a[i][0] += m[j]*dr[0];
      a[j][0] -= m[i]*dr[0];
      a[i][1] += m[j]*dr[1];
      a[j][1] -= m[i]*dr[1];
      a[i][2] += m[j]*dr[2];
      a[j][2] -= m[i]*dr[2];

      return 0;
      }
}
```

The problem with this method is, that the accelerations in MOND do not depend on the chosen coordinate-system and so on the coordinates itself. This would lead to strong unphysical results.
In the MOND case for example the several components would have different values for accelerations that would be affected differently by MOND.
So I decided to calculate the whole acceleration itself, dependent only on the distance from the centre and then split this acceleration into three spatial components.

```
int get_acceleration(unsigned int n,double *m,double **r,double **a){
  unsigned int i,j;
  double dr[3],r2,r1,r3,ddr[3]; /* Hilfsvariablen */
  double a_0, a_rad, dist, Ms, gnewton,a_add;

 for(i=0;i<n;i++)
    for(j=0;j<3;j++)
      a[i][j] = 0;

a_0= 9.980035097e-12 ; /* MONDian limit-acceleration [AU/Day^2] */
Ms= 1.9891E+30;
gnewton=1.487226392E-34; /*Newtons Gravitational constant in AU/kg/Day^2 */

for(i=0;i<(n-1);i++){  /*n = # of Objects */
      dist = sqrt(r[i][0]*r[i][0]+r[i][1]*r[i][1]+r[i][2]*r[i][2]);
      a_rad=gnewton*Ms/(dist*dist);  /*Newtonian Force*/
      a_add=a_rad/2.+sqrt((a_rad/2.)*(a_rad/2.)+a_rad*a_0)
/* Used formula for MONDian acceleration */

      a[i][0] +=-(a_add)*r[i][0]/(dist);
      a[i][1] +=-(a_add)*r[i][1]/(dist);
      a[i][2] +=-(a_add)*r[i][2]/(dist);
    }

.
.
.
.return 0;
}
```

It should be mentioned here that the whole problem has been treated as a two-body-problem. To fix the central mass at the origin of the coordinate-system it has been necessary to set the accelerations acting on the central mass equal to zero.
The modifications due to Λ_- and the Dark-matter-halo have been treated as additional accelerations. So it was possible to calculate these accelerations seperately for every component.

For the acceleration due to Λ_- I used this code

```
int get_acceleration(unsigned int n,double *m,double **r,double **a){
  unsigned int i,j;
  double dr[3],r2,r1,r3,ddr[3]; /* Hilfsvariablen */
  double lambda, c;

lambda= -3.08833565e-22;
c= 173.2644983;  /*Speed of light in AU/Day */

  for(i=0;i<(n-1);i++)
    for(j=i+1;j<n;j++){
      /* Distance between object i and j */
      dr[0] = r[j][0]-r[i][0];
      dr[1] = r[j][1]-r[i][1];
      dr[2] = r[j][2]-r[i][2];
      ddr[0] = dr[0];
      ddr[1] = dr[1];
      ddr[2] = dr[2];

      r2 = dr[0]*dr[0]+dr[1]*dr[1]+dr[2]*dr[2];
      r1 = sqrt(r2);
      r3 = r2*r1;
      dr[0] /= r3;
      dr[1] /= r3;
      dr[2] /= r3;

      a[i][0] += m[j]*dr[0]-lambda*c*c*ddr[0]/3;
      a[i][1] += m[j]*dr[1]-lambda*c*c*ddr[1]/3;
      a[i][2] += m[j]*dr[2]-lambda*c*c*ddr[2]/3;
    }

.
.
.
.return 0;
}
```

For the DM-case the additional constant acceleration has been calculated via $a_{DM} = 2\pi G\rho_0$.

```
int get_acceleration(unsigned int n,double *m,double **r,double **a){
  unsigned int i,j;
  double dr[3],r2,r1,r3,ddr[3]; /* Hilfsvariablen */
  double lambda, c, H2, a_0, a_rad, dist, Ms, gnewton,a_add,rho0;

lambda= -3.08833565e-22;
rho0=1.266301459e+20;
a_0= 9.980035097e-12 ; /* AU/Day^2 */
Ms= 1.9891E+30;
gnewton=1.487226392E-34;
a_add=gnewton*2*PI*rho0;

  for(i=0;i<(n-1);i++)    /*n = # of Objects */
    for(j=i+1;j<n;j++){
      /* Abstand zw. Objekt i und j */
      dr[0] = r[j][0]-r[i][0];
      dr[1] = r[j][1]-r[i][1];
      dr[2] = r[j][2]-r[i][2];
      ddr[0] = dr[0];
      ddr[1] = dr[1];
      ddr[2] = dr[2];

      r2 = dr[0]*dr[0]+dr[1]*dr[1]+dr[2]*dr[2];
      r1 = sqrt(r2);
      r3 = r2*r1;
      dr[0] /= r3;
      dr[1] /= r3;
      dr[2] /= r3;

      a[i][0] += m[j]*dr[0];
      a[i][1] += m[j]*dr[1];
      a[i][2] += m[j]*dr[2];


      dist = sqrt(r[i][0]*r[i][0]+r[i][1]*r[i][1]+r[i][2]*r[i][2]);

      a[i][0] +=-(a_add)*r[i][0]/(dist);
      a[i][1] +=-(a_add)*r[i][1]/(dist);
      a[i][2] +=-(a_add)*r[i][2]/(dist);
    }.
.
.
.return 0;
}
```